

# **A coupling of hydrologic and hydraulic models appropriate for the fast floods of the Gardon river basin (France).**

O. Laganier<sup>1</sup>, P.A. Ayrat<sup>1</sup>, D. Salze<sup>1</sup> and S. Sauvagnargues<sup>1</sup>

[1]{Ecole des Mines d'Alès, Laboratoire de Génie de l'Environnement Industriel et des Risques Industriels et Naturels, Alès, France}

Correspondence to: pierre-alain.ayral@mines-ales.fr

## **Abstract**

Mediterranean catchments are regularly affected by fast and flash floods. Numerous hydrologic models were developed, and allow to reconstruct these floods. However, these approaches often concern average size basins, of a few hundred km<sup>2</sup>. At more important scales (> 1 000 km<sup>2</sup>), a coupling of hydrologic and hydraulic models appears to be an adapted solution. This study has for first objective the evaluation of the performances of a coupling of models for the floods hydrographs modelling. Then, secondly, the coupling results are compared with those of other modellings options. These comparisons aim at clearing up the following points: 1) Is a simplified propagation model (Lag&Route) as efficient as a full hydraulic model for the modelling of the hydrographs of the intermediary-downstream part of the stream? 2) Is adding lateral inflows necessary for all studied events? 3) What is the impact of the qualities of upstream modellings feeding the coupling? The coupling combines the SCS-LR hydrologic model of the ATHYS platform, and the MASCARET 1D hydraulic model, based on full equations of Saint-Venant. It is applied to the Gardon river basin (2 040 km<sup>2</sup>), in the South of France. The performances are analyzed for 7 recent events. The obtained coupling results are satisfactory. Furthermore, this coupling seems well adapted for flood and inundation forecasting.

## **1 Introduction**

Fast and flash floods in the Mediterranean area are well-known for their importance and violence. They are characterized by very brutal reactions by rivers, with specific discharges rates sometimes greater than 20 m<sup>3</sup>/s/km<sup>2</sup>, and flood water rising very rapidly, generally in a

1 few hours. These reactions are the consequence of extremely rainy episodes, for which  
2 cumulated rainfall can reach values superior to 500 mm in 24h, with intensities sometimes  
3 superior to 100 mm/h. In France, the southeast regions are frequently affected. The last major  
4 events are the ones that affected the Aude river in November 1999 (Gaume et al., 2004), the  
5 Gard area in September 2002 (Delrieu et al., 2005), and the Var area in June 2010 (Martin,  
6 2010). Each of these events took many human lives, and generated damages for amounts of  
7 between 500 million and more than one billion euros.

8 The literature informs a set of satisfactory solutions for the floods modelling of Mediterranean  
9 rivers, at the scale of small or medium-sized catchments (lower than some hundred km<sup>2</sup>).  
10 Numerous adapted hydrologic models were proposed, but there is not, at the moment, a clear  
11 consensus as to a preferential approach (Hapuarachchi et al., 2011). TOPMODEL and its  
12 derivatives (Saulnier and Le Lay, 2009; Vincendon et al., 2010), or else the models based on  
13 the SCS theory (see for example: Bouvier et al., 2004; Gaume et al., 2004; Sangati and Borga,  
14 2009), are among some of the best known.

15 These hydrologic models are not adapted for the modelling of large Mediterranean streams,  
16 draining areas of the order of 1 000 km<sup>2</sup> or more. At these scales, overflowing can be  
17 important, because of the widening of the floodplain. The issues at stake are often more  
18 numerous there than in the upstream parts: cities, roads along the streams... At present, the  
19 flood warning services in charge of flood forecasting in the southeast of France, use and  
20 develop propagation models, which allow to forecast with a few hours in advance, water  
21 levels and discharges reached at points of interest. Besides the water levels and discharges  
22 forecasting at every points of the river, a complementary approach could propose a forecast of  
23 areas which could be flooded (Claudet and Bouvier, 2004). For this purpose, a hydraulic  
24 model based on the Saint-Venant equations or on simplifications of these equations, such as  
25 the diffusive wave and the kinematic wave, is necessary.

26 This hydraulic model, applied to the intermediary-downstream part of the river, must be fed.  
27 If inflows are obtained by hydrologic modelling, this is called a coupling of hydrologic and  
28 hydraulic models. Some examples of coupling were already detailed in the literature (see for  
29 example: Knebl et al., 2005; Whiteaker et al., 2006; Lian et al., 2007; Biancamaria et al.,  
30 2009; Bonnifait et al., 2009; Montanari et al., 2009; Mejia and Reed, 2011; Kim et al., 2012;  
31 Lerat et al., 2012). To our knowledge, a single application concerns a catchment prone to fast  
32 floods: the study of Bonnifait et al. (2009), which propose a coupling of the hydrologic n-

1 TOPMODELS model, with the CARIMA hydraulic model. The coupling is used to  
2 reconstitute the major event of September 2002, at the scale of the Gardon river catchment (2  
3 040 km<sup>2</sup>), in the south of France.

4 This study details the construction and the performances of a coupling of hydrologic and  
5 hydraulic models, also applied to the Gardon river basin. The proposed coupling is  
6 unidirectional. A one dimension hydraulic model based on the full Saint-Venant equations is  
7 used on the intermediary-downstream part of the Gardon river. It is fed by 50 upstream and  
8 lateral inflows. These inflows are modelled with a distributed, conceptual and events-based  
9 hydrologic model. The coupling results are analyzed for 7 recent events, of medium  
10 importance, according to the discharges data recorded by 5 hydrometric stations of the  
11 catchment.

12 An analysis in two phases is proposed. A first part estimates the qualities of the coupling  
13 modellings. Then, secondly, comparisons with the performances of other modelling options  
14 are carried out. These comparisons aim at bringing elements of responses to the following  
15 questionings:

16 - Is a simplified propagation model as effective as a full 1D hydraulic model for the modelling  
17 of the discharges of the intermediary-downstream part of the Gardon river?  
18 - Is the use of the coupling justified for all events, or can a simple hydraulic model, without  
19 lateral inflows, be sufficient in some cases?

20 - What is the impact of the qualities of the hydrologic modellings at upstream entry of the  
21 hydraulic model?

22 The different modellings are estimated at 5 stations of the catchment. The analysis concerns  
23 only the floods hydrographs. Other interesting contributions of the coupling, as for example  
24 the reconstruction of the flooded areas, are not analyzed in this study, but offer interesting  
25 perspectives.

26 This article is organized as follows. Part two provides a description of the Gardon catchment,  
27 the hydrologic data used, and the events studied. Part three describes the strategy for  
28 implementing the coupling approach, the hydrologic and hydraulic models, and the  
29 parameters adjustment. Part four details the coupling results, and the results of the  
30 comparisons with the other modelling options. Finally, the article ends with a discussion.

## 1    2    **Study area and flood events modelled**

### 2    2.1    **The Gardon catchment**

3    The Gardon River is a major tributary of the downstream part of the Rhône River, located in  
4    the southeast of France (Fig. 1). Its watershed area is 2040 km<sup>2</sup> at the confluence. The source  
5    of the Gardon River is in the Cevennes, a low mountain range with a 1699 m peak, the *Pic de*  
6    *Finiels*. It contains two main upstream reaches, the *Gardon d'Alès* and the *Gardon d'Anduze*,  
7    and a single downstream reach. The *Gardon d'Alès* and *Gardon d'Anduze* meet a few  
8    kilometres upstream from the village of Ners, in the intermediate part of the catchment.

9    The upstream and downstream parts of the Gardon river basin have very different features. In  
10   the upstream part, the river system has many branches, and a landscape with steep-sided  
11   valleys and steeply-sloped hillsides. In some places, slopes are greater than 50%. From a  
12   geological point of view, this area is essentially made up of former grounds of primary age,  
13   with a preponderance of schist and granites, and a lower proportion of sandstone. The  
14   vegetation consists of oaks and chestnut trees, with a great number of conifers at high altitude.  
15   Downstream from Alès and Anduze, the valleys widen and create alluvial plains with deposits  
16   of the Quaternary, which in some places extend over several kilometres. The widest point is  
17   in the *Gardonnenque* plain. The river system is simplified, because it crosses softer  
18   formations of the secondary era (limestone, marls, and sandstone). Some elements of relief  
19   remain, which rarely exceed 200 m. The landscape is dominated by scrubland and cropland.  
20   This zone of plains ends with the Gardon gorges, which are profoundly dug in limestone, and  
21   in some places rise up to about 100 m. The Gardon gorges stretch over about twenty  
22   kilometres. The River Gardon tributaries have a highly karstic nature in these places.  
23   Downstream from the gorges, the River Gardon crosses a zone of alluvial deposits from the  
24   River Rhone. The floodplain widens, although less than in the *Gardonnenque* plain.

25   There are some moderate size cities (Fig. 1) in this catchment, which is predominantly rural.  
26   Located in the intermediate part of the catchment, Alès is the biggest city with a current  
27   population of slightly more than 40,000 inhabitants. Total population in the catchment was  
28   estimated to be 191,000 inhabitants in 2006 (orig.cg-gard.fr), of which about 25% live in  
29   flood risk areas.

30   Climate in the Gardon watershed is typically Mediterranean. It is characterized by sometimes  
31   very intense and violent rainy events, which generally occur in the autumn. These events

1 cause fast floods (flash floods in the upstream parts), which sometimes have tragic  
2 consequences. The catastrophic event in September 2002, which affected the River Gardon  
3 and the nearby Cèze and Vidourle river basins, is still in everyone's mind. Values cited in the  
4 literature demonstrate how exceptional it was (Delrieu et al., 2005). Cumulated rainfall  
5 between 600 and 700 mm in 24 hours was observed in the triangle linking the cities of Alès,  
6 Anduze, and Ners, which is the current record in the region. Peak specific discharges superior  
7 to  $20 \text{ m}^3/\text{s}/\text{km}^2$  were recorded in certain sub-catchments (Delrieu et al., 2005). There were 23  
8 victims, and damage was estimated to be 1.2 billion euros for the whole area (Sauvagnargues-  
9 Lesage and Simonet, 2004; Ruin et al., 2008).

## 10 **2.2 Hydrological data and events studied**

11 Discharge data from five hydrometric stations in the catchment were used. Figure 1 indicates  
12 the locations of these stations. Table 1 provides data on the surface area drained and the  
13 catchment outlet distances for each station. Rainfall radar images at 1-km resolution were also  
14 analysed. They come from two Météo-France radars, located near the catchment, in the cities  
15 of Bollène and Manduel (Fig. 1). The radar images were corrected beforehand according to  
16 the rain gauge network measurements, using CALAMAR<sup>®</sup> software (Ayrat et al., 2005;  
17 Thierion et al., 2011). These discharge and rainfall data were supplied by the regional flood  
18 warning service SPC-GD ("*Service de Prévision des Crues Grand Delta*"), and have a 5-  
19 minute time step. This fine time step is used for modelling, as it is well adapted to the fast  
20 kinetics of events in this catchment.

21 For this study, seven events were analysed, which occurred between 2005 and 2011. These  
22 events were among the most important ones during the period, for which hydrological data  
23 are the most complete. Table 2 summarises some of their characteristics. Total rainfall  
24 upstream to Russan varied between 140 mm for event n°6 and 370 mm for event n°7. Peak  
25 flows in this station were between  $700 \text{ m}^3/\text{s}$  (event n°5) and  $1420$   
26  $\text{m}^3/\text{s}$  (event n°4). Figure 2 provides data for the cumulated rainfall distribution in the  
27 catchment for each event. Two general trends can be seen:

- 28 - For events n°1 and 5, cumulated rainfall is more significant in the intermediary-  
29 downstream part of the catchment. Table 2 shows for these two cases an increase in  
30 the volume at the downstream stations, indicating the proportionally important  
31 contribution of lateral inflows in these zones.

1 - For events n°2, 3, 4, 6, and 7, cumulated rainfall was more important in the upstream  
2 part of the catchment. This distribution of rain is the one most frequently observed  
3 (Jacq, 1994), because the Cevennes mountains amplify the rainfall. The volume  
4 increased between the upstream stations and the station of Ners, in a way, however,  
5 rather different according to the event. Lateral inflows were the most important for  
6 events n°6 and 7. Volumes diminished between Ners and Russan for events n°2, 3,  
7 and 4. This decrease can be understood in terms of karstic losses in the river bed,  
8 and/or rating curves inaccuracies. It also corresponds to insignificant contributions of  
9 lateral inflows between both stations.

10 Some remarks concerning the hydrological data of these events must be made. Hydrographs  
11 at the Alès station are not available for events n°1 and 2, because the station rating curve is  
12 not valid for these periods. The rating curve at Remoulins is very uncertain, and its discharge  
13 data were not used in this study. Finally, in the case of event n°6, rainfall radar data are  
14 missing at the beginning of the event. They were completed by rain gauge measurements  
15 using inverse distance interpolation techniques.

### 16 **3 The coupling of models: choices and definitions**

17 In this part, we present the chosen coupling approach, and the models we used. Then, the  
18 application of the coupling to the Gardon catchment is detailed.

#### 19 **3.1 The choice of the type of coupling**

20 Two major strategies of coupling of hydrologic and hydraulic models are proposed in the  
21 literature (Lian et al., 2007; Lerat, 2009; Mejia and Reed, 2011): the unidirectional coupling  
22 (also called external) and the bidirectional coupling (internal coupling). In the first case, the  
23 information is exchanged in one direction only, from the hydrologic model to the hydraulic  
24 model. Hydrographs obtained with the hydrologic model feed the hydraulic model, which is  
25 used at a second stage. It is the simplest strategy of coupling, and the most frequently used  
26 (Lerat, 2009). For the bidirectional coupling, the hydraulic model interacts with the  
27 hydrologic model, allowing a more realistic modelling at confluences (backwater effects are  
28 taken into account). At each time step of the modelling, both models are made consistent,  
29 according to a complex procedure. An example of this approach of coupling is detailed by  
30 Kim et al. (2012).

1 In our study, an external coupling of models was chosen. Several criteria motivated this  
2 choice. Firstly, this type of coupling is more flexible: the models can be easily changed, if the  
3 need appears (Whiteaker et al., 2006). This fact is important, because there is still no clear  
4 consensus on a preferential approach for hydrologic modelling of flash floods, as stated by  
5 Hapuarachchi et al. (2011). So, if a more relevant hydrologic model is developed in the  
6 coming years, it can be easily integrated in the coupling, simply by replacing the former  
7 model. Furthermore, the implementation of a bidirectional coupling on the scale of a  
8 catchment such as the one of the Gardon river, appears to be complicated, and little adapted to  
9 the operational vocation wished for the tool. According to Lerat (2009), the applications of  
10 bidirectional coupling are limited to watersheds of restricted areas, of some km<sup>2</sup> to dozens of  
11 km<sup>2</sup>, because of the numerical complexity of the approach. The durations of modellings, and  
12 numerical instabilities, are more important than for a unidirectional coupling.

### 13 **3.2 The choice of the models**

14 The external coupling combines a hydrologic model and a hydraulic model. In this section,  
15 the choice of both models is detailed.

16 As indicated in the introduction, the coupling must be able to estimate discharges, water  
17 levels, and flooded areas, at every point of the stream. These spatially distributed informations  
18 would be of a particular interest for flood forecasting. So, the used coupling has to contain a  
19 hydraulic model based on the Saint-Venant equations, or on simplified approximations of  
20 these equations. Propagation models, such as the Muskingum (McCarthy, 1938) or  
21 Lag&Route (Linsley, 1949) models, are dismissed, because they do not allow to estimate the  
22 flooded areas. However, discretized versions of these two approaches, as for example the  
23 Muskingum-Cunge model (Miller and Cunge, 1975), would be, a priori, satisfactory for the  
24 modelling of discharges in each point of the reach.

25 This first choice makes, the question of the dimension, and of the simplification level of the  
26 equations of the hydraulic model, arises. The hydraulic models can be at one, two, or three  
27 dimensions. The 3D models are rather infrequent in the literature, and their field of  
28 application is restricted to very short reaches, lower than one kilometer. At the complete scale  
29 of a stream, 1D or 2D models are used. The 1D models constitute the oldest approach, but are  
30 still in wide use and development (Horritt and Bates, 2002; Cook and Merwade, 2009). They  
31 can be completed by storage areas for a finer representation of overflowing. The 2D models

1 are more realistic, being released from the constraint of axial flow. They present, as main  
2 weak points, a heavy implementation requiring a large number of data (fine topography, local  
3 roughnesses...), as well as important calculation times, which limits even at present their  
4 interest for an operational use. So, we favor a 1D hydraulic model.

5 It can be based on the full Saint-Venant equations, or on simplifications of these latter: the  
6 kinematic wave and the diffusive wave. According to Ponce et al. (1978), the use of the  
7 kinematic wave is valid for streams with steep slopes (around 0.01 m/m), and in areas where  
8 the slope is lower (around 0.0001 m/m), but then in the limited case of slow floods. The  
9 Gardon river, subjected to fast kinetics floods, and with slopes around 0.001 m/m in its  
10 downstream part, seems little enough adapted to this option. The hypothesis of the less  
11 restrictive diffusive wave seems a priori more satisfactory. Moussa and Bocquillon (2009)  
12 apply a model based on this approximation to the Lez catchment, neighbouring the Gardon  
13 river basin, and obtain satisfactory results. A hydraulic model based on the full Saint-Venant  
14 equations requires fine topographic data, and its calculation time is a priori more important.  
15 However, it remains interesting for an operational purpose. So, a 1D hydraulic model based  
16 on the full Saint-Venant equations, or on the simplification of the diffusive wave, seems to be  
17 adapted to the context of the study. We choose a 1D hydraulic model based on the Saint-  
18 Venant equations.

19 This hydraulic model is fed by hydrologic modellings of lateral and upstream inflows. To  
20 satisfy the operational issue, a hydrologic model containing few parameters, with short  
21 calculation times, is favored. Also, it must be adapted to the context of floods of  
22 Mediterranean catchments. In particular, studies on Mediterranean basins showed clear  
23 improvements of modellings when a rainfall data spatially distributed is used in entrance of  
24 the hydrologic model (Saulnier and Le Lay, 2009; Sangati and Borga, 2009; Sangati et al.,  
25 2009; Anquetin et al., 2010; Zoccatelli et al., 2010; Tramblay et al., 2011). Thus, we choose a  
26 conceptual and distributed model, based on a simplified but physically based description of  
27 the catchment, synonym of rapidity.

28 The coupling uses the SCS-LR hydrologic model implemented in the ATHYS modelling  
29 platform (<http://www.athys-soft.org>), and the MASCARET one-dimensional hydraulic  
30 modelling code, based on full Saint-Venant equations. The ATHYS platform is developed by  
31 the IRD (*"Institute of Research for Development"*), and the MASCARET code by EDF  
32 (*"Electricité De France"*—French Electric Company), and the CETMEF (*"Centre d'Etudes*

1 *Techniques Maritimes et Fluviales*”). Both tools, which will be described in the following  
2 section, are open-source.

### 3 **3.3 Description of the models**

#### 4 **3.3.1 SCS-LR hydrologic model**

5 The SCS-LR model combines a runoff model adapted from the Soil Conservation Service  
6 (SCS) and a Lag and Route model (LR) based on a cascade of linear reservoirs. It is an  
7 events-based, distributed, conceptual model with reservoirs, based on a discretization of the  
8 catchment in regular square cells. It has been used in many studies on Mediterranean  
9 watersheds of limited area, in particular concerning the *Gardon d’Anduze* river basin (Bouvier  
10 et al., 2004; Bouvier et al., 2006; Marchandise, 2007; Marchandise and Viel, 2009; Coustau,  
11 2011; Tramblay et al., 2011). It proves to be successful for modelling typical floods on  
12 Mediterranean watersheds, particularly compared with other models (Bouvier et al., 2006;  
13 Marchandise, 2007; Coustau, 2011).

14 The SCS runoff model associates a time variable runoff coefficient  $C(t)$  with every grid cell,  
15 which depends on the cumulated rainfall  $P(t)$ , and on an  $S$  parameter, characterising the initial  
16 water deficit in the catchment area:

$$C(t) = \left( \frac{P(t) - 0.2S}{P(t) + 0.8S} \right) \left( 2 - \frac{P(t) - 0.2S}{P(t) + 0.8S} \right)$$

17 (1)

18 with  $P(t)$  and  $S$  in mm,  $C(t)$  in %.

19 This runoff coefficient increases with the cumulated rainfall. To represent its decrease during  
20 period without rains, a reduction of  $P(t)$  is added:

$$\frac{dP(t)}{dt} = Pb(t) - dsP(t)$$

21 (2)

22 where  $Pb(t)$  is the instantaneous precipitation in mm/h, and  $ds$  a coefficient ( $\text{h}^{-1}$ ).

23 Finally, the runoff  $R(t)$  of the cell (mm/h) is expressed as:

$$R(t) = C(t).Pb(t)$$

1 (3)

2 The LR routing model is based on the definition of a propagation time  $T_m$  and of a diffusion  
3 time  $K_m$  for each cell  $m$ , estimated from the cell to outlet distances  $l_m$ :

$$T_m = \frac{l_m}{V_0}$$

4 (4)

$$K_m = K_0 T_m$$

5 (5)

6 where  $V_0$  is the speed of propagation (m/s), and  $K_0$  a coefficient without dimension. The  
7 elementary discharge  $q(t)$  at outlet, corresponding to the propagation of the runoff  $R(t_0)$   
8 generated at the cell  $m$  at time  $t_0$ , is:

$$q(t) = 0$$

9 if  $t < t_0 + T_m$

$$q(t) = \frac{R(t_0)}{K_m} \exp\left(-\frac{t - (t_0 + T_m)}{K_m}\right) B$$

10 if  $t > t_0 + T_m$

11 (6)

12 where  $B$  is the cell surface.

13 Finally, the complete flood hydrograph is obtained by adding all the contributions of the cells,  
14 at each time. A five-minute time step is used for modelling.

15 This model is a simplified version of the complete SCS-LR model of the ATHYS platform,  
16 and is identical to the one used by Tramblay et al. (2011). In this version, the contribution of  
17 delayed flows is ignored. Tramblay et al. (2011) showed that it gives satisfactory results for  
18 16 events at the Anduze station. Besides this last observation, this version was chosen because  
19 it has a low number of adjustment parameters, which is an important criterion for flood  
20 forecasting. The model contains four parameters, for which values must be defined:  $S$ ,  $ds$ ,  $V_0$   
21 and  $K_0$ . The adjustment is detailed in section 3.6.

### 1 3.3.2 The MASCARET hydraulic model

2 MASCARET is the one-dimensional hydraulic modelling code used for developing the  
3 hydraulic model. It can be used to calculate steady and unsteady flows in fluvial and  
4 transcritical systems. It is based on full Saint-Venant equations, composed of the continuity  
5 equation:

$$\frac{\partial Q}{\partial x} + \frac{\partial A}{\partial t} = q_l$$

6 (7)

7 and of the dynamic equation:

$$\frac{\partial Q}{\partial t} + \frac{\partial}{\partial x} \left( \beta \frac{Q^2}{A} \right) + gA \left( \frac{\partial y}{\partial x} \right) + gA(S_f - S_0) = 0$$

8 (8)

9 where  $Q$  is the discharge ( $\text{m}^3/\text{s}$ ),  $x$  the longitudinal distance (m),  $A$  the wetted area ( $\text{m}^2$ ),  $q_l$  the  
10 lateral inflows by meter ( $\text{m}^2/\text{s}$ ),  $\beta$  the Boussinesq coefficient, without dimension,  
11 characterizing the variations of speed in the cross-section,  $g$  the gravity ( $\text{m}/\text{s}^2$ ),  $y$  the water  
12 depth (m),  $S_f$  the friction slope (m/m), and  $S_0$  the bed slope (m/m). Using the Manning-  
13 Strickler expression,  $S_f$  can be written:

$$S_f = \frac{Q^2}{K_s^2 A^2 R_h^{4/3}}$$

14 (9)

15 with  $K_s$  the Strickler coefficient ( $\text{m}^{1/3}/\text{s}$ ) which characterizes flow resistance, and  $R_h$  the  
16 hydraulic mean radius (m) such as  $R_h = A/P$ , with  $P$  the wetted perimeter (m).

17 The 1D Saint-Venant models are subjected to several hypotheses:

- 18 - The flow follows a privileged direction;
- 19 - The density of water is supposed constant;
- 20 - The pressure is distributed in a hydrostatic way;
- 21 - The slope of the stream is moderated (lower than 0.1 m/m).

22 The 1D Saint-Venant equations are based on a discretization of topography in cross sections  
23 (Samuels, 1990). In the face of hydraulic structures (weirs, dams...), they are replaced locally  
24 by adapted hydraulic equations. Some examples are given in EDF-CETMEF (2011).

1 Numerical techniques are used for solving the equations. Two schemes, explicit and implicit,  
2 are implemented in the MASCARET code, and are at the user choice.

3 The model has several adjustment parameters: the  $K_s$  Strickler coefficient ( $m^{1/3}/s$ ), the values  
4 of friction losses, and the coefficients of the hydraulic structures equations.

### 5 **3.4 Application of the coupling to the Gardon river basin**

6 Figure 3 shows how the coupling of models was implemented in the studied catchment. The  
7 MASCARET hydraulic model is applied from the Anduze and Alès stations up to the  
8 Remoulins station. Floodplains widen considerably downstream from both stations, leading to  
9 important overflowing during strong floods, which justify the employment of a hydraulic  
10 model. The studied reach includes the gorges zone, which is very influential during extreme  
11 events, in particular during the one of September 2002 (see Fig. 1).

12 The hydraulic model consists of three reaches. Both upstream reaches correspond to the  
13 downstream parts of the *Gardon d'Anduze* and *Gardon d'Alès*, which are 14.5 and 12.5 kms  
14 long. The downstream reach connects the confluence with the Remoulins station, and is 55.2  
15 kms long. The total extent of the hydraulic model is 82.2 kms. There are about 50 inflows,  
16 with two major upstream inflows (the Alès and Anduze sub-catchments), and 48 lateral  
17 inflows (Fig. 3). Lateral inflows were defined on the basis of a minimum threshold area of 1  
18  $km^2$ . The average area of lateral sub-catchments is 20  $km^2$ , for a median value of 5  $km^2$ . Sub-  
19 catchments n°2, 20, 26, 28, and 39 have an area greater than 50  $km^2$ , the maximum being 203  
20  $km^2$  for inflow n°39. All in all, the selected lateral sub-catchments cover 92% of the area  
21 between both upstream stations and the Remoulins station.

### 22 **3.5 Models characteristics**

23 The 50 lateral inflows are modelled with the SCS-LR model, in a simplified version (see Sect.  
24 3.3.1). The cell grid of the model is built from a Digital Elevation Model (DEM) of the IGN's  
25 BD ALTI® (“*Institut national de l'information géographique et forestière*”). The cell size is  
26 of 100 × 100 m. This resolution is particularly well adapted to the smallest lateral sub-  
27 catchments. The flow paths between each cell, allowing the cell to outlet distances ( $l_m$ ) to be  
28 evaluated, were forced according to the river polylines of the catchment, on the basis of the  
29 IGN's BD CARTHAGE®. This processing seemed necessary in the intermediate-downstream

1 part of the Gardon catchment, where low slopes falsify flow paths, and the areas really  
2 drained.

3 The rainfall data in entrance of the model are the CALAMAR<sup>®</sup> data at 1-km resolution,  
4 evoked in section 2.2. These CALAMAR<sup>®</sup> data are interpolated in each cell of the model,  
5 according to the Thiessen method.

6 As indicated above, the hydraulic model contains three main reaches (Fig. 3), connected by a  
7 zone of confluence. The topographic data in entrance of the hydraulic model are cross  
8 sections. They are identical to those of the study of Bonnifait et al. (2009). They had been  
9 collected with the SPC-GD and with the SMAGE (“*Syndicat Mixte d’Aménagement des*  
10 *Gardons*”). Missing in the gorges sector, the authors had to complete them by means of  
11 1:25000 maps. All in all, the hydraulic model used contains 161 cross sections. To limit  
12 miscalculations, additional sections were interpolated. The spacing of cross sections varies  
13 from 10 to 50 m depending on zones.

14 Bridges and weirs of the Gardon river were taken into account in the model. The geometries  
15 of the bridges which were recovered, were integrated into cross sections. Coefficients of  
16 friction losses were associated to them. Weirs are modelled by means of specific hydraulic  
17 equations (see EDF-CETMEF, 2011), containing two parameters: the weirs crest elevation,  
18 and a discharge coefficient. All in all, the model contains 15 bridges and 18 weirs.

19 The initial condition of the hydraulic model is a water line, characterizing the base flow. In  
20 this study, it is identical for all the events, and corresponds to a constant discharge of 5 m<sup>3</sup>/s  
21 injected into both upstream stations.

22 The time step of SCS-LR modellings is of 5 minutes. In the case of the hydraulic model, the  
23 explicit resolution scheme chosen requires a very fine a time step for modelling, of 0.1s in this  
24 case. The model outputs are then sampled at a 5 minutes time step.

### 25 **3.6 Models parameters adjustments**

26 The SCS-LR hydrologic model, as indicated previously, contains four parameters to be  
27 adjusted. An identical strategy to that adopted by Trambly et al. (2011) is chosen: the  $S$  and  
28  $V_0$  parameters are adjusted for each event, and the  $ds$  and  $K_0$  parameters are fixed to a constant  
29 value. The model is particularly sensitive to the  $S$  values. The  $V_0$  parameter influences  
30 essentially the value and the time of arrival of the peak. Modellings of about twenty events at

1 Anduze, carried out in parallel to this study, were sometimes improved very clearly after  
2 calibration of this parameter. It is also calibrated, after this observation. Concerning the  $ds$   
3 and  $K_0$  parameters, the values used by Tramblay et al. (2011) are used, i.e.:  $ds = 0.4$  and  $K_0 =$   
4  $1.5$ .

5 The  $S$  and  $V_0$  parameters are calibrated according to observed hydrographs at the Anduze  
6 station. For this purpose, the simplex iterative algorithm (Nelder and Mead, 1965),  
7 implemented in the ATHYS platform, is used. The algorithm is based on the maximization of  
8 a quality criterion of the modelling. In this particular case, the Nash criterion (Nash and  
9 Sutcliffe, 1970) is used:

$$Nash = 1 - \frac{\sum_{i=1}^T (Q_{OBS,i} - Q_{MOD,i})^2}{\sum_{i=1}^T (Q_{OBS,i} - \overline{Q_{OBS}})^2}$$

10 (10)

11 where  $T$  is the event duration, and  $Q_{OBS,i}$  and  $Q_{MOD,i}$  ( $m^3/s$ ) are the observed and modeled  
12 discharges at time step  $i$ .

13 The calibration domain includes only discharges superior to  $50 m^3/s$ , to limit the influence of  
14 low values. However, in the case of event n°5, for which peak flow does not reach this  
15 threshold at Anduze (Tab. 2), the calibration procedure was applied to discharges superior to  
16  $10 m^3/s$ .

17 The  $S$  and  $V_0$  values obtained after calibration are then used for the modelling of the 49 other  
18 inflows (the Alès sub-catchment and the 48 lateral inflows). The  $ds$  and  $K_0$  fixed values are  
19 equally employed.

20 Table 3 indicates the parameter values calibrated at Anduze for the 7 events studied. The  $S$   
21 parameter values follow a coherent trend. For events arising just after the summer season, the  
22  $S$  parameter is high, characterising an important water deficit. On the contrary, for events in  
23 November-December, the values are lower, since rainy events at the beginning of autumn  
24 have contributed in a more or less significant way to refilling the catchment. The  $V_0$  values  
25 are rather variable, but coherent with the classically observed speeds. The performance of the  
26 hydrologic modelling is described in section 4.1.1.

27 The parameters of the hydraulic model are the Strickler coefficients  $K_s$ , the friction losses  
28 coefficients, and the coefficients of the hydraulic equations associated with weirs. The friction  
29 losses were defined according to the values of literature. Both parameters of the weirs

1 equation, i.e. the weirs crest elevation and the discharge coefficient, respectively derive  
2 respectively from the IGN's BD TOPO<sup>®</sup>, and from the literature.

3 The  $K_s$  Strickler coefficients of the hydraulic model were empirically adjusted. The procedure  
4 consisted in reducing as much as possible the time differences between the observed and  
5 simulated peaks, and between the observed and simulated beginning of flood rises, at the  
6 three stations in Ners, Russan, and Remoulins. The beginning of the flood rise is identified as  
7 the first discharge value exceeding 50 m<sup>3</sup>/s. Several sets of the Strickler coefficient were  
8 estimated, for which values vary from 15 to 30 in the river bed, and from 10 to 15 in  
9 floodplain. The adjustment procedure was applied to event n°3. The hydrographs observed at  
10 Anduze and Alès, and the lateral inflows modelled are the boundaries conditions of the  
11 hydraulic model. This event was chosen because the lateral inflow contributions were weak  
12 (Tab. 2), and had little influence in terms of shifting the peak times.

13 The best set considered a Strickler coefficient of 25 in the river bed, except in the gorges,  
14 where it was 30, and 10 in the floodplain. This parameterisation is very satisfactory in terms  
15 of peak flow timing. The peak modelled for event n°3 was 5 minutes late at Ners, 5 minutes  
16 early at Russan, and on time at Remoulins. The peak propagation times from one station to  
17 another seem to be entirely satisfactory. Performance was a bit less satisfactory concerning  
18 the beginning of flood rise times, with an average delay of one hour at the three stations. This  
19 parameter set was used for all the other events in the study.

20 In this way, only two parameters of the coupling ( $S$  and  $V_0$ ) were adjusted for each event, at  
21 the Anduze station. Other parameters and initial conditions remained identical. This  
22 parsimonious criterion makes the coupling very interesting from an operational point of view.

### 23 **3.7 Performance assessment**

24 The performance of the coupling of models was evaluated by analysing discharge data from  
25 five stations in the catchment area, as shown in figure 1. The quality of the hydrologic  
26 modelling was estimated on the basis of hydrographs recorded at Anduze and Alès, and for  
27 lateral inflows according to the differences in volume observed between two consecutive  
28 stations. The performance of the coupling was evaluated at three stations in the downstream  
29 part of the catchment (Ners, Russan, and Remoulins).

30 Three quality indicators were assessed. First, the Nash coefficient, which was already  
31 mentioned in the last section. It provides information on the overall quality of the

1 hydrographs modelled. The other two indices are specific to peak flow. These coefficients are  
2 the relative error for peak flow  $RE_{Q_m}$  (%), and the temporal difference between the observed  
3 and simulated peaks  $\Delta T_{Q_m}$  (min):

$$RE_{Q_m} = \frac{Q_{m_{MOD}} - Q_{m_{OBS}}}{Q_{m_{OBS}}} \times 100$$

4 (11)

$$\Delta T_{Q_m} = T_{m_{MOD}} - T_{m_{OBS}}$$

5 (12)

6 with  $Q_{m_{MOD}}$  and  $Q_{m_{OBS}}$  as the modelled and observed peak flows ( $m^3/s$ ), and  $T_{m_{MOD}}$  and  
7  $T_{m_{OBS}}$  as the corresponding times. A positive  $RE_{Q_m}$  value indicates an overestimation in the  
8 peak modelled, and conversely. The  $\Delta T_{Q_m}$  index is positive when the peak modelled is late,  
9 and negative if it is early. At the Remoulins station, only the  $\Delta T_{Q_m}$  index was estimated,  
10 because the rating curve was too uncertain as indicated above.

## 11 **4 Results**

12 This part presents the obtained results. At first, the coupling of models results are detailed.  
13 Then, comparisons with other modellings options are analyzed.

### 14 **4.1 Coupling results**

#### 15 **4.1.1 Hydrologic modelling of upstream inflows and lateral inflows**

16 The SCS-LR hydrologic modelling results were evaluated at both the Anduze and Alès  
17 stations, and for lateral inflows according to the differences in volumes observed between the  
18 downstream stations.

19 Table 4 presents the modelling results at Anduze (the calibration station) and Alès. Events n°1  
20 and n°2 were not provided for the second station, because the rating curve was not valid  
21 during these periods (see Sect. 2.2). Performance was generally satisfactory at Anduze, with  
22 Nash values varying from 0.53 to 0.91. A similar range of values was observed by Trambly  
23 et al. (2011) with the same version of the model, for a 16 event set at Anduze. At the Alès  
24 station, Nash values were very different from one event to another, indicating qualities  
25 varying from very bad to very good. The Nash index decreased for all events compared with  
26 the Anduze values. Nash values are sometimes negative, reflecting a very bad adaptation of

1 parameters calibrated at Anduze. The peak evaluation indices were, however, rather  
2 satisfactory at both stations. Peak error was between 0 and  $\pm 25\%$ , and the  $\Delta T_{Qm}$  index  
3 between 0 and  $\pm 30$  minutes, for 5 events. Only events n°6 and n°7 present major errors.  
4 These two cases contain several peaks, and a secondary peak was identified as the main peak  
5 by the model. Some hydrographs modelled at Anduze and Alès are represented in figure 4.  
6 Flood fall is in general rather poorly represented, particularly for winter or end of autumn  
7 events. This observation is directly attributable to the choice of a simplified version of SCS-  
8 LR model.

9 Table 5 compares the differences in volumes observed between the downstream stations, with  
10 the volumes generated by lateral inflows included between these stations, estimated with  
11 SCS-LR. The differences in volumes at Ners cannot be estimated for events n°1 and 2, and  
12 the hydrographs at Alès were missing as indicated above. There appears to be a tendency to  
13 underestimate the volumes modelled for lateral inflows along the Alès / Anduze - Ners  
14 reaches, and on the contrary a tendency to overestimate them for those along the Ners-Russan  
15 reach. There is volume compensation at the Russan station, where the total volume modelled  
16 for lateral inflows since Alès and Anduze is closer to the differences in volumes observed,  
17 than at the Ners station. It is difficult to propose a physical interpretation of these inflow  
18 differences between both sections. The rather marked karstic functioning of the downstream  
19 sub-catchments, for which the hydrologic model is not in theory well adapted, the  
20 uncertainties linked to the rating curves, and a bad adaptation of parameters calibrated at  
21 Anduze, are possible explanations.

#### 22 **4.1.2 Coupling performance at the downstream stations**

23 The results of the coupled models at the Ners, Russan, and Remoulins stations are presented  
24 in Table 6. Coefficients are generally good for the selected range of events. The Nash index is  
25 between 0.61 and 0.92 at Ners, and between 0.72 and 0.97 at Russan. Event n°3 presents the  
26 highest values at both stations, whereas event n°2 has the lowest. The  $REQ_m$  index has  
27 satisfactory values between 0 and  $\pm 15\%$  for most events. However, peaks for events n°1, 5,  
28 and 7 at the Ners station, present more important errors, with the highest peak overestimation  
29 of 39% for event n°7. The  $\Delta T_{Qm}$  index was equal to or less than 30 minutes for five events at  
30 Ners, and for four at Russan and Remoulins, which characterises good peak flow timing, and  
31 confirms the hydraulic model parameterisation described in Section 3.6. However, this

1 coefficient is very high at three stations for event n°7: the delay for the peak modelled is more  
2 than twenty hours.

3 Results presented in Table 6 also bring to light an improvement in the Nash values at Russan,  
4 compared with those at Ners, for all events. The average increase was 13% between both  
5 stations. There is a twofold explanation for this observation. First, the improvement in the  
6 modelling of events n°2, 3, and 4 (varying from +0.05 to +0.11) for which lateral inflows at  
7 the section Ners-Russan are insignificant or of little importance (Table 5), indicate that the  
8 hydraulic model is better adapted at Russan, and/or a more valid rating curve at this station. It  
9 is necessary to specify that the Ners station is located only 4 kms downstream from the  
10 confluence, which complicates the hydraulic model. It is also possible that the topographic  
11 data of the hydraulic model are more precise near Russan. The second explanation concerns  
12 the others events, and particularly those for which lateral inflows are proportionally important  
13 (events n°1 and n°5). It was previously noted that the total volume of lateral inflows from  
14 Alès and Anduze is more satisfactory at Russan than at Ners, as there is a compensation at the  
15 most downstream station. This more correct estimation also seems to be responsible for the  
16 improved results of the coupled models at Russan. The Nash values increased for events n°1  
17 and 5 by +0.11 and +0.20. If this trend toward improvement is clear for the Nash coefficient,  
18 it is barely obvious for the indices concerning peak flow.

## 19 **4.2 Comparison with other modelling options**

20 The coupling of models results at the Ners, Russan and Remoulins stations, are now  
21 compared with those of other modelling options. These comparisons are going to allow us to  
22 bring elements of responses to the following questionings:

- 23 - Is a simplified propagation model as relevant as a hydraulic model based on full Saint-  
24 Venant equations, for the estimation of the discharges at the Ners, Russan and  
25 Remoulins stations?
- 26 - Is the consideration of lateral inflows justified for all the events? In other words, is the  
27 choice of a coupling appropriate, or could a simple hydraulic model without lateral  
28 inflows suit?
- 29 - What is the impact of the quality of modellings injected at Anduze and Alès on the  
30 coupling results in the downstream?

1 For greater clarity, the abbreviation  $\text{COUPL}_{\text{MOD}}$  identifies the coupling previously detailed.  
2 The following comparisons are analyzed.

3 At first (Sect. 4.2.1), we try to estimate the influence of a simplified conceptualization for  
4 flood wave propagations. For this purpose, the  $\text{COUPL}_{\text{MOD}}$  results are compared with those  
5 obtained with the Lag&Route routing scheme of the SCS-LR model. This option is noted LR.  
6 Upstream and lateral inflows are identical in both cases. The only differences between both  
7 options concern:

- 8 - The resolute equations: full Saint-Venant equations in the case of  $\text{COUPL}_{\text{MOD}}$ , and  
9 physically based but simplified equations in the case of LR (see Sect. 3.3);
- 10 - The representation of the river bed: it is very detailed in the case of  $\text{COUPL}_{\text{MOD}}$  (cross  
11 sections), simplified in the case of LR (square cells).

12 Secondly, we assess the interest of adding lateral inflows (Sect. 4.2.2). The  $\text{COUPL}_{\text{MOD}}$   
13 results are compared with those obtained with the simple hydraulic model, without lateral  
14 inflows. This option is noted  $\text{SV}_{\text{MOD}}$ . Upstream entries are identical for both options: they are  
15 hydrologic modellings.

16 Then, in the third section (Sect. 4.2.3), we try to estimate the impact of upstream entries on  
17 the hydraulic model results. For that purpose, the  $\text{COUPL}_{\text{MOD}}$  results are compared with those  
18 of the coupling, integrating the observed (recorded) upstream entrances, and thus, perfect.  
19 This option is noted  $\text{COUPL}_{\text{OBS}}$ . The lateral inflows are identical for both approaches: they  
20 are SCS-LR modellings.

21 Finally, in the fourth part (Sect. 4.2.4), we directly estimate the importance of taking into  
22 account lateral inflows, with regard to the importance of the quality modellings for upstream  
23 inflows. The  $\text{COUPL}_{\text{MOD}}$  results are compared with those of the  $\text{SV}_{\text{OBS}}$  option. This  $\text{SV}_{\text{OBS}}$   
24 option corresponds to the hydraulic model without lateral inflows, fed upstream by the  
25 observed hydrographs.

#### 26 **4.2.1 $\text{COUPL}_{\text{MOD}}$ vs LR: influence of a simplified routing conceptualization**

27 The parameters of the LR routing model,  $V_0$  and  $K_0$  (see Sect. 3.3.1) , are calibrated for each  
28 of 7 events, on the three Alès/Anduze – Ners, Ners – Russan, and Russan – Remoulins  
29 reaches, according to the hydrographs observed at downstream stations. Upstream entries and

1 lateral inflows are identical to those of the COUPL<sub>MOD</sub> modelling. The results of the LR  
2 option are presented in table 7.

3 The Nash indexes vary according to events, between 0.62 and 0.93 at Ners, and between 0.61  
4 and 0.87 at Russan. The RE<sub>Qm</sub> coefficients are globally average. If some values are interesting  
5 (event n°6 at Ners, events n°1 and 7 at Russan), errors on some peaks reach more than 30 %.  
6 In the same way, the  $\Delta T_{Qm}$  indexes are often important, in particular at the Russan station,  
7 where the peak is clearly early for 6 events.

8 At the Ners station, the performances in terms of Nash are equivalent between both options,  
9 even slightly to the advantage of the LR option. At Russan, this option is less successful: five  
10 events present clear degradations of the Nash indexes. Concerning the RE<sub>Qm</sub> index,  
11 consequent gaps are observed for events n°2, 3 and 4, at both stations. Some peaks are  
12 however reproduced in a equivalent way by both options. It is difficult to identify a global  
13 trend concerning the  $\Delta T_{Qm}$  index. There are so many improvements as degradations of this  
14 index at Ners; at Russan, the COUPL<sub>MOD</sub> option is more successful; at Remoulins, the results  
15 are equivalent for five events, but benefit the LR option for events n°1 and 6.

16 Some hydrographs at the Russan station are detailed in figure 5. The performances of both  
17 options are close in the case of events n°1 and 7. Concerning this last event, the Nash index is  
18 slightly degraded with the LR option (0.79 with COUPL<sub>MOD</sub>; 0.74 with LR). The recessions  
19 between peaks, as well as first peak, are better modelled with COUPL<sub>MOD</sub>. Concerning the  
20 remaining two events, peaks modelled with LR are rather clearly underestimated, and early.  
21 The COUPL<sub>MOD</sub> modelling seems more satisfactory in these cases.

22 So, it is difficult to conclude on the impact of a simplified routing conceptualization on the  
23 downstream results. The performances of both options, COUPL<sub>MOD</sub> and LR, are globally  
24 equivalent at Ners; the  $\Delta T_{Qm}$  indexes calculated at Remoulins are also often rather close. At  
25 Russan, it appears for four cases a clear degradation of modellings with the LR option (events  
26 n°2, 3, 4 and 5). It is maybe the location of the Russan station, just above the Gardon gorges,  
27 which explains this finding. In this sector, the river bed narrows brutally: this configuration is  
28 finely reproduced in the hydraulic model, while the LR option does not take this into account.

#### 29 **4.2.2 COUPL<sub>MOD</sub> vs SV<sub>MOD</sub>: influence of adding lateral inflows**

30 The SV<sub>MOD</sub> option corresponds to the simple hydraulic model, without lateral inflows, fed  
31 upstream by hydrographs modelled with SCS-LR. A comparison with COUPL<sub>MOD</sub> informs

1 the interest of adding lateral inflows for the modelling. The results of the  $SV_{MOD}$  option are  
2 indicated in table 8.

3 The performances with this option are very variable according to the events. The Nash  
4 indexes are rather good for events n°3, 4 and 7, moderates for n°2 and 6, and very bad for n°1  
5 and 5. In the same way, the  $RE_{Qm}$  and  $\Delta T_{Qm}$  indexes are very bad for events n°1 and 5, but  
6 also for event n°7 (except the  $RE_{Qm}$  index at Russan), and, to a lesser extent however, for  
7 event n°6. They are rather satisfactory for the remaining three events.

8 The comparison with the  $COUPL_{MOD}$  modelling informs significant differences according to  
9 the events. It seems these differences between both options depend on the cumulated rainfall  
10 spatial distribution (Fig. 2). The indexes obtained for events n°2, 3 and 4, are rather little  
11 different from those achieved with  $COUPL_{MOD}$ . A light improvement of Nash at Ners is noted  
12 in the case of event n°4, when the lateral inflows are added (0.75 vs 0.80). These three events  
13 present more significant rainfall in the upstream part of the catchment, and rather little  
14 important contributions of lateral inflows (see Tab. 5). This fact explains the absence of  
15 notable gaps between both options.

16 By contrast, for events n°1, 5, and to a lesser extent for event n°6, important differences are  
17 observed: the  $COUPL_{MOD}$  results are more satisfactory than those of  $SV_{MOD}$ , for all indexes.  
18 For example, Nash of event n°5 evolve from -1.05 at Ners and -0.73 at Russan with the  
19  $SV_{MOD}$  option, to respectively 0.68 and 0.88 when lateral inflows are taken into account. So,  
20 adding these seems necessary for the good modelling of these three events. Again, this finding  
21 can be explained by the rainfall spatial distribution during these events: for n°1 and 5, the  
22 strongest rains were measured in the intermediary-downstream part of the catchment, causing  
23 very important laterals inflows responses, proportionally to the flows at Anduze and Alès  
24 (Tab. 2 and Tab. 5); in the case of event n°6, the highest cumulated rainfall are observed in  
25 the upstream part of the catchment, but inflows of the intermediary-downstream part react in a  
26 consequent way.

27 Finally, in the case of event n°7, modellings degrade when lateral inflows are added. The  
28 Nash indexes with the  $SV_{MOD}$  option are over of +0.06 at Ners, and +0.09 at Russan. This  
29 lesser quality of the  $COUPL_{MOD}$  results is understandable by the errors of the hydrologic  
30 model at Alès and Anduze: the second peak of this event is rather widely overestimated in  
31 both stations (see Fig. 4). Adding lateral inflows amplifies this error in the downstream, and  
32 as a consequence modellings are of less good quality. This case of degradation is the only one

1 observed when lateral inflows are added. The  $\Delta T_{Q_m}$  indexes remain rather close according to  
2 both options, being very bad: it is also the consequence of upstream errors.

3 Figure 6 details observed and modelled hydrographs with  $COUPL_{MOD}$  and  $SV_{MOD}$  at Russan,  
4 for events n°1, 3, 6 and 7. The differences between both options are little visible in the case of  
5 event n°3: Nash indexes are very close. However, the  $COUPL_{MOD}$  modelling estimates the  
6 peak more finely. Conversely, differences are very important for event n°1. The  $SV_{MOD}$   
7 option underestimates the event rather widely. Flood rises are much delayed, and the second  
8 peak is widely underestimated. A less significant underestimation is also observed for event  
9 n°6. Finally, in the case of event n°7, the  $SV_{MOD}$  option is the most satisfactory. Adding  
10 lateral inflows, overestimated on the Ners-Russan reach (see Tab. 5), explains the too  
11 premature increases preceding the last two peaks, and the too important values of these, in the  
12 case of the  $COUPL_{MOD}$  modelling.

13 To summarize, we can say that the interest of adding lateral inflows depends essentially on  
14 the rainfall spatial distribution of the event. However, adding lateral inflows can also  
15 contribute to the degradation of modellings, by worsening the errors on upstream entries (case  
16 of event n°7).

### 17 **4.2.3 $COUPL_{MOD}$ vs $COUPL_{OBS}$ : influence of the upstream injected** 18 **hydrographs**

19 The  $COUPL_{OBS}$  option is identical to the  $COUPL_{MOD}$  option, except concerning upstream  
20 entries to the hydraulic model, which are in this case the observed hydrographs. So, the  
21  $COUPL_{OBS}/COUPL_{MOD}$  comparison allows to estimate the impact of the qualities of  
22 modellings injected at Anduze and Alès on the coupling results at the downstream. In the  
23 cases of events n°1 and 2, for which the rating curve at Alès is not adapted, hydrographs  
24 modelled at this station are taken into account. The results of the  $COUPL_{OBS}$  option are  
25 indicated in table 9.

26 Globally with this option, the indexes are rather satisfactory for all the events. The Nash  
27 coefficients vary between 0.63 and 0.98 at Ners, and are higher than 0.85 at Russan. The  
28  $RE_{Q_m}$  index is sometimes very good. Some gaps higher than 20 % are however noted at Ners.  
29 Peaks are generally well synchronized. Rather important gaps are raised for some cases: event  
30 n°1, event n°6 at Russan and Remoulins, and event n°7 at Remoulins. They appear to be due  
31 to hydrologic modellings errors on lateral inflows, rather than to the hydraulic model. The

1 presented case of event n°3, is the case which was used to the adjustment of the  $K_s$  parameters  
2 of the hydraulic model (see Sect. 3.6).

3 As in the previous section, gaps in performance according to both modelling options are very  
4 different from one event to another. There are very few differences between the results of  
5 COUPL<sub>MOD</sub> and COUPL<sub>OBS</sub> for events n°1, 3 and 5. Only the Nash indexes at Ners in the case  
6 of event n°5, and the  $\Delta T_{Qm}$  coefficients at Ners for event n°1, present reasonable gaps. Again,  
7 the rainfall spatial distribution is an explanation of this observation. The lateral inflows were  
8 consequent during events n°1 and 5, minimizing the importance of hydrographs injected  
9 upstream to the hydraulic model. So, the modelling accuracy of lateral inflows is not  
10 fundamental for these two cases. Concerning event n°3, it is the good modelling of  
11 hydrographs at Alès and Anduze (respective Nash indexes of 0.91 and 0.89, see Tab.4) which  
12 explains the low gap between both options at the Ners, Russan and Remoulins stations. The  
13 lateral inflows play a secondary role during this event (see Tab. 5).

14 Three other events, n°2, 4 and 6, present clear increases of the Nash indexes, and limited  
15 differences for the  $RE_{Qm}$  and  $\Delta T_{Qm}$  indexes when hydrographs observed upstream are injected  
16 (COUPL<sub>OBS</sub> option). The strongest Nash increase is observed in the case of event n°6 at Ners  
17 (Nash of 0.64 with COUPL<sub>MOD</sub> vs 0.95 with COUPL<sub>OBS</sub>, an improvement of almost 50 %).  
18 This increase is explained by a better representation of flood rises and falls. For these three  
19 events, the quality of modellings at Alès and Anduze is important for the improvement in the  
20 Nash values at the downstream: this can be attributed to the strong contributions of upstream  
21 inflows, considering the flowed out volumes at the downstream stations (see Tab. 2).  
22 However, the two others indexes do not present clear improvements.

23 Finally, event n°7 constitutes, as already observed in the previous section, a special case. All  
24 the indexes are improved with the COUPL<sub>OBS</sub> option. Previously observed errors of  $\Delta T_{Qm}$  are  
25 widely corrected: the main peak is well identified this time.

26 Some modellings according to both options, at the Ners station, are presented in figure 7. In  
27 the case of event n°5, the results do not differ much: the quality of the modelling of upstream  
28 inflows has not got much impact. The differences are clearer concerning the three other  
29 events. In the case of events n°4 and 6, the flood rises and falls are better reproduced with the  
30 COUPL<sub>OBS</sub> option: modellings at Anduze and Alès underestimate them (see Fig. 4 for event  
31 n°4). However, the peak is better reproduced with COUPL<sub>MOD</sub> for event n°6: it is the  
32 combined result of overestimations of peaks at Anduze and Alès (see the  $RE_{Qm}$  index, Tab. 4),

1 and of an underestimate of the lateral inflows upstream to Ners (see Tab. 5), which  
2 compensates these errors upstream. In the case of event n°7, the improvements of the indexes  
3 are understandable by a better estimation of peaks and flood fall, with the COUPL<sub>OBS</sub> option.  
4 It is interesting to note the important role of both upstream catchments on flood falls, which  
5 are, except for event n°5, far better modelled when upstream entries are the observed data.

6 To summarize, the results show again the important role of the rainfall spatial distribution.  
7 Events with rains essentially located in the upstream part, present the most important  
8 improvements when the observed data are taken into account. However, these improvements  
9 are more debatable concerning the reconstruction of peaks: rather often, the RE<sub>Qm</sub> and ΔT<sub>Qm</sub>  
10 indexes are little different according to both options. Only event n°7 presents an improvement  
11 of all the indexes with COUPL<sub>OBS</sub>.

#### 12 **4.2.4 COUPL<sub>MOD</sub> vs SV<sub>OBS</sub>: direct comparison of the impact of the quality of** 13 **upstream injected hydrographs, vs the importance of the lateral inflows**

14 In this section, the interest of adding lateral inflows is directly confronted with the impact of  
15 modellings at the upstream entries. For that purpose, the results of the hydraulic model  
16 without lateral inflows, fed by the observed data at Anduze and Alès, are compared with the  
17 COUPL<sub>MOD</sub> results, at the three downstream stations. This modelling option is noted SV<sub>OBS</sub>,  
18 and its results are presented in table 10.

19 Again, the indexes values, and the gaps with regard to the COUPL<sub>MOD</sub> modelling, are very  
20 variable according to the events. As previously evoked, the complete coupling is necessary  
21 for events n°1 and 5. Important gaps between both options are noted, the results of the SV<sub>OBS</sub>  
22 option being unsatisfactory. There are few differences in the case of event n°3, for which  
23 lateral inflows are not much consequent, and SCS-LR modellings are very good at Alès and  
24 Anduze. In the case of events n°2, 4, 6 and 7, improvements of the Nash indexes are noticed.  
25 Concerning the two other indexes, they are equivalent for events n°2 and 4, clearly degraded  
26 with SV<sub>OBS</sub> for event n°6, and improved with this same option for event n°7. These trends  
27 appear to the modelled hydrographs, presented, for some events, in figure 8.

28 For event n°1, gaps are consequent. The SV<sub>OBS</sub> option clearly underestimates the hydrograph.  
29 Peaks are also underestimated with the coupling. In the case of event n°2, gaps are more  
30 reduced. The peak is reproduced in a very satisfactory way with both options. The gaps in  
31 terms of Nash (0.78 for SV<sub>OBS</sub> vs 0.61 for COUPL<sub>MOD</sub>) are hard to see: we can barely say that

1 the flood rise and fall are slightly better reproduced with the  $SV_{OBS}$  option. In the case of  
2 event n°6, this last option is also more satisfactory on flood rise and fall, but less interesting  
3 for the reproduction of the peak: the addition of lateral inflows is necessary for its good  
4 estimation. Finally, in the case of event n°7, the  $SV_{OBS}$  option is the most satisfactory, except  
5 for the evaluation of the last peak.

6 Thus, the  $SV_{OBS}/COUPL_{MOD}$  comparison ends in contrasted findings according to the events.  
7 Nash is improved or equivalent for five events with  $SV_{OBS}$ , which indicates, in these cases,  
8 the importance of the quality of modellings upstream to the hydraulic model. The indexes  
9 relative to peaks are however often equivalent for both options. Adding lateral inflows  
10 appears to be necessary for events n°1, 5, and for the good modelling of the peak of event n°6.

## 11 **5 Discussion**

12 The presented results show that the coupling of models is an interesting tool for the modelling  
13 of the hydrographs of the Gardon river at the downstream stations. In this part, two points are  
14 discussed: the choice of the hydrologic model parameters of the ungauged lateral inflows, and  
15 the use and the interests of the coupling for floods forecasting.

### 16 **5.1 Concerning the SCS-LR hydrologic model parameters of the ungauged** 17 **inflows**

18 In this study, the SCS-LR hydrologic model parameters calibrated at Anduze are used for the  
19 modellings of the others sub-catchments feeding the hydraulic model, gauged (Alès), or not  
20 (the 48 lateral inflows). With this simplified approach, the performances of the coupling are  
21 satisfactory at the Ners, Russan and Remoulins stations. However, they could be improved,  
22 using better adapted parameters.

23 Naturally, the parameters cannot be calibrated on ungauged catchments. For the lateral  
24 inflows modelling, regionalization approaches of the parameters seem adapted (see examples  
25 in: Merz and Blöschl, 2004; McIntyre et al., 2005; Parajka et al., 2005; Oudin et al., 2008;  
26 Masih et al., 2010; Oudin et al., 2010; Garambois, 2012). These methods are based on  
27 parameters calibrated on gauged catchments. The literature details three regionalization  
28 approaches:

- 29 - The regressive approaches. Regressions between the parameters calibrated on gauged  
30 catchments and physical and climatic descriptors are established. The set of

1 parameters of the ungauged catchment is known according to the value of the  
2 descriptor of the basin. These methods require a large number of gauged catchments,  
3 to cover a wide range of descriptors values.

4 - The approaches based on spatial proximity. The parameters calibrated on the closest  
5 catchments are averaged, then directly used for the target ungauged catchment. This  
6 approach is based on the hypothesis that nearby catchments have similar hydrological  
7 reactions, because of the relative homogeneity of the physical and climatic  
8 characteristics. It approximates the strategy used in this study.

9 - The approaches by physical similarity. The sets calibrated on the closest gauged  
10 catchments, but this time in the sense of the physical and climatic characteristics, are  
11 averaged then used for the ungauged basin. The similarity between catchments is  
12 quantified by means of an index.

13 According to Oudin et al. (2008), there is still no clear consensus for a preferential  
14 regionalization method. According to Garambois (2012), the regionalization methods by  
15 similarity, defined from soils characteristics, are particularly relevant for catchments of the  
16 Cévennes area.

17 Methods of correction of modellings for ungauged catchments were also developed. Artigue  
18 (2012) provides an example, applied to ungauged sub-catchments of the Gardon river basin.  
19 The author proposes a correction of his neural networks model results, by means of a law  
20 based on the ungauged basins areas and the estimated maximal specific discharges. This  
21 correction strategy allows to obtain realistic modellings.

22 These solutions constitute an appropriate way to improve the hydrologic modellings of sub-  
23 catchments, and thus the coupling of models results.

## 24 **5.2 Use of the coupling for flood forecasting**

25 As previously evoked, the elaborate coupling of models is a priori adapted for flash flood  
26 forecasting, and overflowing associated. In this section, we indicate the existing approaches to  
27 define both parameters of the coupling before the beginning of the event. Then, we detail the  
28 modelling of the inundated areas.

29 The coupling of models contains two parameters which must be adjusted for each event:  $S$   
30 and  $V_0$ . In this study, these two parameters were calibrated, what is obviously impossible in a  
31 forecasting context: the values of both parameters must be defined beforehand. For that

1 purpose, the literature describes several possible options. A first approach consists in using  
2 one or several state indicators of the catchment, as for example the soil moisture, the base  
3 flow... Regressions are established between the parameters calibrated for a range of events,  
4 and the corresponding indicators values. The parameters for an upcoming event are then  
5 known, according to the indicator value of the day. This option was analyzed for the  $S$   
6 parameter of the SCS-LR model, at the scale of the Gardon d'Anduze catchment  
7 (Marchandise and Viel, 2009; Trambly et al., 2011). These authors show that the  $Hu2$  index  
8 calculated every day by the SIM model of Météo-France (Habets et al., 2008), and estimating  
9 the soil moisture of the root layer (between 10 and 190 cm), is particularly interesting to  
10 estimate the  $S$  parameter.

11 A second approach was recently developed, and is described by Coustau (2011) and Coustau  
12 et al. (2013). These authors propose assimilation techniques of discharges for the estimation  
13 of the  $S$  and  $V_0$  parameters of the SCS-LR model. They show that an assimilation in the first  
14 few hours of the flood allows to obtain parameters supplying good results, according to their  
15 tests on the Lez river catchment (neighbor of the Gardon river basin). This option is also  
16 interesting.

17 Thus, it would be advisable for a use of the coupling in an objective of flood forecasting, to  
18 predetermine the parameters according to one of these two approaches. These parameters  
19 must be then regionalized on the ungauged catchments, as we mentioned earlier.

20 The coupling is a priori relevant for the modelling of the flooded areas. However, the 1D  
21 hydraulic model in its current form, is little adapted. Indeed, in the floodplain, the flows are  
22 strongly multidirectional, and do not satisfy the hypothesis of 1D flow. For a fine modelling  
23 of overflowing, it would be advisable to use a 2D model, or to complete the 1D model with  
24 storage areas. The choice of a 1D model rather than a 2D approach had previously been  
25 justified (see Sect. 3.2). The 2D model requires very fine data, and its calculation times are  
26 more important, which is a limiting constraint for a use in operational forecast. Furthermore,  
27 studies comparing 1D and 2D models, indicate close results with both options, for the  
28 modelling of inundated areas (Horritt and Bates, 2002; Aureli et al., 2006; Besnard and  
29 Goutal, 2011). However, in the case of the study of Aureli et al. (2006), the 2D model allows  
30 a more realistic representation of overflowing during the first hours of the event. Besnard and  
31 Goutal (2011) proposes a MASCARET model with storage areas, applied to the Garonne

1 river, in the southwest of France. The authors indicate the importance of the links between  
2 storages areas, which must be defined in a fine way for the good modelling of overflowing.

3 So, adding storage areas to the hydraulic model, appears to be a necessary step for the  
4 coupling of models relevance for major events, such as the one of September 2002.

## 5 **6 Summary and conclusions**

6 This study showed that a coupling of hydrologic and hydraulic models is adapted for  
7 modelling the fast floods of the Gardon river basin. At the downstream stations of the  
8 catchment, the Nash values are included between 0.61 and 0.97, reflecting qualities rated as  
9 rather good to excellent. The coefficients specific to peak flows are also satisfactory. For the  
10 most part of the studied events, the relative error for peak flow ( $RE_{Q_m}$ ) is included between  
11  $\pm 15\%$ , and the temporal difference ( $\Delta T_{Q_m}$ ) is lower or of the order of 30 minutes.

12 A comparison with other modelling strategies was made, and allowed to provide responses to  
13 the questioning asked in introduction and at section 4.2.

14 At first, we are interested in the contribution of a full hydraulic model for the discharges  
15 estimation, compared with a simplified Lag&Route routing model. Close results were  
16 observed. The coupling is slightly more successful at the Russan station, and even rather  
17 clearly for four events. At Ners and Remoulins, both options seem rather equivalent. So, a  
18 simplified Lag&Route model can suit for discharges routing on the intermediary-downstream  
19 part of the Gardon river. However, contrary to the hydraulic model, it does not allow to  
20 estimate flooded areas.

21 The second interrogation concerned the interest of adding lateral inflows. For this purpose,  
22 the coupling results were compared with those of the  $SV_{MOD}$  option (hydraulic model without  
23 lateral inflows). The gaps between both options differ rather clearly according to events. The  
24 rainfall spatial distribution during the event is a key element. When cumulated rainfalls are  
25 more important in the intermediary-downstream part of the catchment (case of events n°1, 5,  
26 and to a lesser extent for event n°6), adding lateral inflows is necessary: the coupling is  
27 clearly more successful than the  $SV_{MOD}$  option. On the other hand, when rains are rather  
28 centered on sub-catchments upstream to the hydraulic model, the gaps between both options  
29 are rather low (case of events n°2, 3 and 4). Then, the lateral inflows are not necessary. The  
30 case of event n°7 constitutes an interesting feature: it is the only event for which the  $SV_{MOD}$

1 option is the most successful. This fact is understandable by an amplification of the errors of  
2 both modellings at upstream entries to the hydraulic model, when lateral inflows are added.

3 Thirdly, the impact of the qualities of modellings at upstream entries to the hydraulic model  
4 was estimated. For that purpose, the coupling results were compared with those of the  
5 COUPL<sub>OBS</sub> option (identical coupling, but with the recorded hydrographs injected at Alès and  
6 Anduze). Even there, the rainfall spatial distribution during the event is very influential. The  
7 results of both options are very close in the case of events n°1 and 5, for which rains were  
8 scarce in the upstream, but also for event n°3. Concerning this last case, the absence of  
9 significant improvements is understandable by the very good quality of the hydrologic  
10 modellings at Anduze and Alès. The COUPL<sub>OBS</sub> modelling is more satisfactory, in terms of  
11 Nash, for 4 others episodes. These events with heavy rains upstream require good hydrologic  
12 modellings upstream. In the cases of events n°2, 3 and 4, the differences are however of little  
13 significance concerning the RE<sub>Qm</sub> and  $\Delta T_{Qm}$  indexes.

14 A last comparison estimated the gaps between the SV<sub>OBS</sub> results (hydraulic model without  
15 lateral inflows, with observed upstream entries) and those of the coupling. In the case of  
16 events n°1 and 5, the coupling is clearly more successful than the SV<sub>OBS</sub> option. It shows that  
17 adding lateral inflows is more important than a satisfactory hydrologic modelling at Alès and  
18 Anduze. The SV<sub>OBS</sub> option is more successful in terms of Nash, for events n°2, 4, 6 and 7.  
19 The improvements concern especially flood rises and falls. The differences are hardly  
20 noticeable for peaks, in the case of events n°2 and 4; the modelled peak is more satisfactory  
21 with the coupling, in the case of event n°6.

22 If the coupling results are satisfactory, they could be improved thanks to better hydrologic  
23 modellings of lateral inflows. For this purpose, methods of correction of modellings (Artigue,  
24 2012) or of parameters regionalization (Garambois, 2012), were estimated for Mediterranean  
25 basins and seem relevant for this studied case.

26 Finally, this coupling of models turns out very interesting for floods forecasting. However, the  
27 problem of the estimation of the coupling parameters before the event, arises. For this  
28 purpose, approaches of assimilation of data (Coustau, 2011; Coustau et al., 2013) or of  
29 estimation of the parameters according to state indicators of the catchment (Marchandise and  
30 Viel, 2009; Trambly et al., 2010; Trambly et al., 2011), are relevant. Furthermore, the 1D  
31 hydraulic model, completed by storage areas, should be very interesting for the inundated area

1 modelling during major events, as the one of September, 2002. The continuation of works  
2 will address these two aspects.

### 3 **Acknowledgments**

4 The authors thank Yann Laborda, from SPC-GD, for supplying the hydrological data useful to  
5 this study, and its sensible advice. Thanks are also presented to Fabrice Zaoui, from EDF, for  
6 its advice relating to the MASCARET code. Thanks to Guy Delrieu, from LTHE  
7 (*Laboratoire d'étude des Transferts en Hydrologie et Environnement*), to have supplied river  
8 cross sections, necessary for this study. Finally, thanks to Gilles Rocquelain, Fabrice Cebron  
9 and Marie-Christine Germain, from *BRL Ingénierie*, for their advice and remarks.

### 10 **References**

11 Anquetin, S., Braud, I., Vannier, O., Viallet, P., Boudevillain, B., Creutin, J.-D., and Manus,  
12 C.: Sensitivity of the hydrological response to the variability of rainfall fields and soils for the  
13 Gard 2002 flash-flood event, *J. Hydrol.*, 394, 134-147, doi:10.1016/j.jhydrol.2010.07.002  
14 2010.

15 Artigue, G.: Prédiction des crues éclair par réseaux de neurones : généralisation aux bassins  
16 non jaugés, Ph.D., Université Montpellier II, Montpellier, France, 318 pp., 2012.

17 Aureli, F., Mignosa, P., Ziveri, C., and Maranzoni, A.: Fully-2D and *quasi*-2D modeling of  
18 flooding scenarios due to embankment failure, *River Flow 2006 – Ferreira, Alves, Leal &*  
19 *Cardoso (eds), Taylor & Francis Group, London, England, 1473-1482, 2006.*

20 Ayral, P.A., Sauvagnargues-Lesage, S., and Bressand, F.: Contribution à la spatialisation du  
21 modèle opérationnel de prédiction des crues éclair Alhtair, *Études de Géographie Physique*,  
22 32, 75-97, 2005.

23 Besnard, A., and Goutal, N.: Comparaison de modèles 1D à casiers et 2D pour la  
24 modélisation hydraulique d'une plaine d'inondation – Cas de la Garonne entre Tonneins et La  
25 Réole, *Houille Blanche*, 3-2011, 42-47, doi:10.1051/lhb/2011031, 2011.

26 Biancamaria, S., Bates, P.D., Boone, A., and Mognard, N.M.: Large-scale coupled hydrologic  
27 and hydraulic modelling of the Orb river in Siberia, *J. Hydrol.*, 379, 136-150,  
28 doi:10.1016/j.jhydrol.2009.09.054, 2009.

29 Bonnifait, L., Delrieu, G., Le Lay, M., and Boudevillain, B., Masson, A., Belleudy, P.,  
30 Gaume, E., Saulnier, G.M.: Distributed hydrologic and hydraulic modelling with radar

1 rainfall input: reconstruction of the 8-9 September 2002 catastrophic flood event in the Gard  
2 region, France, *Adv. Water Res.*, 32, 1077-1089, doi:10.1016/j.advwatres.2009.03.007, 2009.

3 Bouvier, C., Marchandise, A., Lequien, A., Brunet, P., and Crespy, A.: Distributed  
4 rainfall/runoff modelling of September 2002 flood in two southern France river basins,  
5 BALWOIS International Scientific Conference, Ohrid, Republic of Macedonia, 25-29 May  
6 2004, 2004.

7 Bouvier, C., Ayral, P.A., Brunet, P., Crespy, A., Marchandise, A., and Martin C.: Recent  
8 advances in rainfall-runoff modelling: extrapolation to extreme floods in southern France,  
9 Proceedings of the AMHY-FRIEND International Workshop on Hydrological Extremes,  
10 University of Calabria, Cosenza, Italy, 3-4 May 2006, 229-238, 2006.

11 Claudet, R., and Bouvier, C.: Outils de prévision des crues rapides : les besoins de l'alerte et  
12 du suivi en temps réel, Colloque SHF « Crues méditerranéennes », Nîmes, France, June 2004,  
13 105-112, 2004.

14 Cook, A., and Merwade, V.: Effect of topographic data, geometric configuration and  
15 modeling approach on flood inundation mapping, *J. Hydrol.*, 377, 131-142, 2009.

16 Coustau, M.: Contribution à la prévision des crues sur le bassin du Lez : modélisation de la  
17 relation pluie-débit en zone karstique et impact de l'assimilation de débits, Ph.D., Université  
18 Montpellier II, Montpellier, France, 234 pp., 2011.

19 Coustau, M., Ricci, S., Borrell-Estupina, V., Bouvier, C., and Thual, O.: Benefits and  
20 limitations of data assimilation for discharge forecasting using an event-based rainfall-runoff  
21 model, *Nat. Hazard. Earth Sys.*, 13, 583-596, doi:10.5194/nhess-13-583-2013, 2013.

22 Delrieu, G., Ducrocq, V., Gaume, E., Nicol, J., Payrastre, O., Yates, E., Kirstetter, P.E.,  
23 Andrieu, H., Ayral, P.A., Bouvier, C., Creutin, J.D., Livet, M., Anquetin, S., Lang, M.,  
24 Neppel, L., Obled, C., Parent-du-Châtelet, J., Saulnier, G.M., Walpersdorf, A., and Wobrock,  
25 W.: The catastrophic flood event of 8-9 September 2002 in the Gard region, France: A first  
26 case study for the Cévennes-Vivarais Mediterranean Hydrometeorological Observatory, *J.*  
27 *Hydrometeorol.*, 6, 34-52, 2005.

28 EDF-CETMEF: MASCARET v7.1 Note de principe, 152 pp., 2011.

1 Gaume, E., Livet, M., Desbordes, M., and Villeneuve, J.P.: Hydrological analysis of the river  
2 Aude, France, flash flood on 12 and 13 November 1999, *J. Hydrol.*, 286, 135-154,  
3 doi:10.1016/j.jhydrol.2003.09.015, 2004.

4 Garambois, P.A.: Étude régionale des crues éclair de l'arc méditerranéen français ;  
5 élaboration de méthodologies de transfert à des bassins versants non jaugés, Ph.D., Université  
6 de Toulouse, Toulouse, France, 451 pp., 2012.

7 Habets, F., Boone, A., Champeaux, J.L., Etchevers, P., Franchistéguy, L., Leblois, E.,  
8 Ledoux, E., Le Moigne, P., Martin, E., Morel, S., Noilhan, J., Quintana Segui, P., Rousset-  
9 Regimbeau, F., and Viennot, P.: The SAFRAN-ISBA-MODCOU hydrometeorological model  
10 applied over France, *J. Geophys. Res.*, 113, DO6113, doi:10.1029/2007JD008548, 18 pp.,  
11 2008.

12 Hapuarachchi, H.A.P., Wang, Q.J., and Pagano, T.C.: A review of advances in flash flood  
13 forecasting, *Hydrol. Process.*, 25, 2771-2784, doi:10.1002/hyp.8040, 2011.

14 Horritt, M.S., and Bates, P.D.: Evaluation of 1D and 2D numerical models for predicting river  
15 flood inundation, *J. Hydrol.*, 268, 87-99, 2002.

16 Jacq, V.: Inventaire des situations à précipitations diluviennes sur le Languedoc-Roussillon, la  
17 Provence-Alpes-Cote d'Azur et la Corse – Période 1958-1994, Météo-France S3C/PRO,  
18 France, 190 pp., 1994.

19 Kim, J., Warnock, A., Ivanov, V.Y., and Katopodes, D.: Coupled modeling of hydrologic and  
20 hydrodynamic processes including overland and channel flow, *Adv. Water Resour.*, 37, 104-  
21 126, doi:10.1016/j.advwatres.2011.11.009, 2012.

22 Knebl, M.R., Yang, Z.L., Hutchison, K., and Maidment, D.R.: Regional scale flood modeling  
23 using NEXRAD rainfall, GIS, and HEC-HMS/RAS: a case study for the San Antonio River  
24 Basin Summer 2002 storm event, *J. Environ. Manage.*, 75, 325-336,  
25 doi:10.1016/j.jenvman.2004.11.024, 2005.

26 Lerat, J.: Quels apports hydrologiques pour les modèles hydrauliques? Vers un modèle intégré  
27 de simulation des crues, Ph.D., Université Pierre et Marie Curie, Paris, France, 390 pp., 2009.

28 Lerat, J., Perrin, C., Andréassian, V., Loumagne, C., and Ribstein, P.: Towards robust  
29 methods to couple lumped rainfall-runoff models and hydraulic models: A sensitivity analysis  
30 on the Illinois River, *J. Hydrol.*, 418-419, 123-135, doi:10.1016/j.jhydrol.2009.09.019, 2012.

- 1 Lian, Y., Chan, I.C., Singh, J., Demissie, M., Knapp, V., and Xie, H.: Coupling of hydrologic  
2 and hydraulic models for the Illinois River Basin, *J. Hydrol.*, 344, 210-222,  
3 doi:10.1016/j.jhydrol.2007.08.004, 2007.
- 4 Linsley, R.K., Kohler, M.A., and Paulhus, J.L.H.: *Applied Hydrology*, McGraw-Hill, New  
5 York, USA, 1949.
- 6 Masih, I., Uhlenbrook, S., Maskey, S., and Ahmad, M.D.: Regionalization of a conceptual  
7 rainfall-runoff model based on similarity of the flow duration curve: A case study from the  
8 semi-arid Karkheh basin, Iran, *J. Hydrol.*, 391, 188-201, doi:10.1016/j.jhydrol.2010.07.018,  
9 2010.
- 10 Marchandise, A.: Modélisation hydrologique distribuée sur le Gardon d'Anduze ; étude  
11 comparative de différents modèles pluie-débit, extrapolation de la normale à l'extrême et tests  
12 d'hypothèses sur les processus hydrologiques, Ph.D., Université Montpellier II, Montpellier,  
13 France, 214 pp., 2007.
- 14 Marchandise, A., and Viel, C.: Utilisation des indices d'humidité de la chaîne Safran-Isba-  
15 Modcou de Météo-France pour la vigilance et la prévision opérationnelle des crues, *Houille*  
16 *Blanche*, 6-2009, 35-41, doi:10.1051/lhb/2009075, 2009.
- 17 Martin, C.: Les inondations du 15 Juin 2010 dans le centre Var : réflexion sur un épisode  
18 exceptionnel, *Études de Géographie Physique*, 37, 41-76, 2010.
- 19 McCarthy, G.T.: *The Unit Hydrograph and flood routing*, unpublished manuscript, 1938.
- 20 McIntyre, N., Lee, H., Wheeler, H., Young, A., and Wagener, T.: Ensemble predictions of  
21 runoff in ungauged catchments, *Water Resour. Res.*, 41, W12434,  
22 doi:10.1029/2005WR004289, 2005.
- 23 Mejia, A.I., and Reed, S.M.: Evaluating the effects of parameterized cross section shapes and  
24 simplified routing with a coupled distributed hydrologic and hydraulic model, *J. Hydrol.*, 409,  
25 512-524, doi:10.1016/j.jhydrol.2011.08.050, 2011.
- 26 Merz, R., and Blöschl, G.: Regionalisation of catchment model parameters, *J. Hydrol.*, 287,  
27 95-123, doi:10.1016/j.jhydrol.2003.09.028, 2004.
- 28 Miller, W., and Cunge, J.: Simplified equations of unsteady flow – Unsteady flow in open  
29 channels, ed. K. Mahmood & V. Yevjevich, Vol. 1, Chap. 5, *Water Resour. Publ.*, Fort  
30 Collins, Colorado, 1975.

1 Montanari, M., Hostache, R., Matgen, P., Schumann, G., Pfister, L. and Hoffmann, L.:  
2 Calibration and sequential updating of a coupled hydrologic-hydraulic model using remote  
3 sensing-derived water stages, *Hydrol. Earth Syst. Sc.*, 13, 367-380, 2009.

4 Moussa, R., and Bocquillon, C.: On the use of the diffusive wave for modelling extreme flood  
5 events with overbank flow in the floodplain, *J. Hydrol.*, 374, 116-135,  
6 doi:10.1016/j.jhydrol.2009.06.006, 2009.

7 Nash, J.E., and Sutcliffe, J.V.: River flow forecasting through conceptual models part I – a  
8 discussion of principles, *J. Hydrol.*, 10, 282-290, 1970.

9 Nelder, J., and Mead, R.: A simplex method for function minimization, *Comput. J.*, 7-4, 308-  
10 313, 1965.

11 Oudin, L., Andréassian, V., Perrin, C., Michel, C., and Le Moine, N.: Spatial proximity,  
12 physical similarity, regression and ungaged catchments: A comparison of regionalization  
13 approaches based on 913 French catchments, *Water Resour. Res.*, 44, W03413,  
14 doi:10.1029/2007WR006240, 2008.

15 Oudin, L., Kay, A., Andréassian, V., and Perrin, C.: Are seemingly physically similar  
16 catchments truly hydrologically similar?, *Water Resour. Res.*, 46, W11558,  
17 doi:10.1029/2009WR008887, 2010.

18 Parajka, J., Merz, R., and Blöschl, G.: A comparison of regionalisation methods for catchment  
19 model parameters, *Hydrol. Earth Syst. Sc. Discuss.*, 2, 509-542, 2005.

20 Ponce, V.M., Li, R.M., and Simons, D.B.: Applicability of kinematic and diffusion models, *J.*  
21 *Hydr. Eng. Div.-ASCE*, 104, 353-360, 1978.

22 Ruin, I., Creutin, J.D., Anquetin, S., and Lutoff, C.: Human exposure to flash floods –  
23 Relation between flood parameters and human vulnerability during a storm of September  
24 2002 in Southern France, *J. Hydrol.*, 361, 199-213, doi:10.1016/j.jhydrol.2008.07.044, 2008.

25 Samuels, P.G.: Cross section location in one-dimensional models, *International Conference*  
26 *on river flood hydraulics*, Great Britain, September 17-20<sup>th</sup> 1990, 339-350, 1990.

27 Sangati, M., and Borga, M.: Influence of rainfall spatial resolution on flash flood modelling,  
28 *Nat. Hazard Earth Syst.*, 9, 575-584, 2009.

29 Sangati, M., Borga, M., Rabuffetti, D., and Bechini, R.: Influence of rainfall and soil  
30 properties spatial aggregation on extreme flash flood response modelling: An evaluation

1 based on the Sesia river basin, North Western Italy, *Adv. Water Resour.*, 32, 1090-1106,  
2 doi:10.1016/j.advwatres.2008.12.007, 2009.

3 Saulnier, G.M., and Le Lay, M.: Sensitivity of flash-flood simulations on the volume, the  
4 intensity, and the localization of rainfall in the Cévennes-Vivarais region (France), *Water*  
5 *Resour. Res.*, 45, W10425, doi:10.1029/2008WR006906, 2009.

6 Sauvagnargues-Lesage, S., and Simonet, C.: Retour d'expérience sur la gestion de  
7 l'évènement de Septembre 2002 par les Services de la Sécurité Civile, *Houille Blanche*, 6-  
8 2004, 1-7, 2004.

9 Thierion, V., Ayral, P.A., Geisel, J., Sauvagnargues-Lesage, S., and Payrastre, O.: Grid  
10 technology reliability for flash flood forecasting: End-user assessment, *J. Grid Computing*, 9,  
11 405-422, 2011.

12 Trambly, Y., Bouvier, C., Martin, C., Didon-Lescot, J.F., Todorovik, D., Domergue, J.M.:  
13 Assessment of initial soil moisture conditions for event-based rainfall-runoff modeling, *J.*  
14 *Hydrol.*, 387, 176-187, doi:10.1016/j.jhydrol.2010.04.006, 2010.

15 Trambly, Y., Bouvier, C., Ayral, P.A., and Marchandise, A.: Impact of rainfall spatial  
16 distribution on rainfall-runoff modeling efficiency and initial soil moisture conditions  
17 estimation, *Nat. Hazard. Earth Sys.*, 11, 157-170, doi:10.5194/nhess-11-157-2011, 2011.

18 Vincendon, B., Ducrocq, V., Saulnier, G.M., Bouilloud, L., Chancibault, K., Habets, F. and  
19 Noilhan, J.: Benefit of coupling the ISBA land surface model with a TOPMODEL  
20 hydrological model version dedicated to Mediterranean flash-floods, *J. Hydrol.*, 394, 256-266,  
21 doi:10.1016/j.jhydrol.2010.04.012, 2010.

22 Whiteaker, T.L., Robayo, O., Maidment, D.R., and Obenour, D.: From a NEXRAD rainfall  
23 map to a flood inundation map, *J. Hydrol. Eng.*, 11, 37-45, doi:10.1061/(ASCE)1084-  
24 0699(2006)11:1(37), 2006.

25 Zocatelli, D., Borga, M., Zanon, F., Antonescu, B., and Stancalie, G.: Which rainfall spatial  
26 information for flash flood response modelling? A numerical investigation based on data from  
27 the Carpathian range, Romania, *J. Hydrol.*, 394, 148-161, doi:10.1016/j.jhydrol.2010.07.019,  
28 2010.

29

30

1 Table 1. Drained areas and outlet distances for the five stations.

2

Stations	Drained areas (km <sup>2</sup> )	Outlet distances (km)
Anduze	545	83.7
Alès	315	81.7
Ners	1100	64.3
Russan	1530	45.3
Remoulins	1900	13.9

3

4

5

6

7

8

9

10

11

12

13

14

15

16

17

18

19

1 Table 2. Some key event characteristics. AN, N, and RU stand for the Anduze, Ners, and  
 2 Russan stations. UP groups together both upstream sub-catchments (Anduze and Alès).

3

Event	Period	Mean rainfall (mm)			Runoff volume (Mm <sup>3</sup> )			Peak discharge (m <sup>3</sup> /s)		
		UP	N	RU	UP	N	RU	AN	N	RU
1	05-12/09/05	280	300	320	-	63	99	150	460	850
2	18-22/10/06	210	170	140	-	91	85	1300	1340	1290
3	21-24/10/08	190	180	160	46	52	50	1070	1390	1340
4	01-04/11/08	250	230	190	98	118	113	1040	1290	1420
5	06-09/09/10	90	120	140	2	15	21	20	560	700
6	21-28/12/10	160	150	130	97	126	133	360	730	880
7	02-09/11/11	460	430	370	195	222	229	1070	1120	1300

4

5

6

7

8

9

10

11

12

13

14

15

16

17

1 Table 3.  $S$  and  $V_0$  parameters calibrated at the Anduze station, for the seven events studied.

2

Event	$S$	$V_0$
1	391	1.6
2	238	3.6
3	408	3.1
4	203	3
5	367	1.4
6	108	1.6
7	227	2.7

3

4

5

6

7

8

9

10

11

12

13

14

15

16

17

18

1 Table 4. Hydrologic modelling results. Performance indexes at the Anduze and Alès stations.

2

Event	Anduze			Alès		
	Nash	RE <sub>Qm</sub>	$\Delta T_{Qm}$	Nash	RE <sub>Qm</sub>	$\Delta T_{Qm}$
1	0.72	-11	-15	-	-	-
2	0.87	-10	10	-	-	-
3	0.91	-25	5	0.89	2	25
4	0.90	-20	-5	0.57	-3	25
5	0.53	-6	-5	-4.57	17	30
6	0.68	15	705	-0.50	24	45
7	0.80	-15	1415	-0.25	69	1180

3

4

5

6

7

8

9

10

11

12

13

14

15

16

1 Table 5. Comparison of the differences in volumes ( $\text{Mm}^3$ ) observed between stations ( $V_{\text{OBS}}$ ),  
 2 and lateral inflow volumes estimated with SCS-LR ( $V_{\text{SCS-LR}}$ ), in both sections Anduze / Alès  
 3 (UP) - Ners and Ners - Russan.

4

Event	UP - Ners		Ners – Russan	
	$V_{\text{OBS}}$	$V_{\text{SCS-LR}}$	$V_{\text{OBS}}$	$V_{\text{SCS-LR}}$
1	-	15.0	35.7	39.9
2	-	0.2	0	0.2
3	5.6	2.4	0	0
4	19.4	5.1	0	1.2
5	12.9	9.2	5.7	11.1
6	28.9	7.5	6.4	6.3
7	27.7	18.2	7.1	19.4

5

6

7

8

9

10

11

12

13

14

15

16

17

1 Table 6. Coupling results. Performance indexes at the Ners, Russan and Remoulins stations.

2

Event	Ners			Russan			Remoulins
	Nash	RE <sub>Qm</sub>	$\Delta T_{Qm}$	Nash	RE <sub>Qm</sub>	$\Delta T_{Qm}$	$\Delta T_{Qm}$
1	0.77	-23	-30	0.86	1	-260	-210
2	0.61	4	25	0.72	-4	5	20
3	0.92	3	15	0.97	-3	10	10
4	0.80	1	-20	0.86	-11	-35	-25
5	0.68	-30	-15	0.88	-12	-20	-10
6	0.64	0	90	0.73	-11	55	70
7	0.75	39	1270	0.79	15	1275	1300

3

4

5

6

7

8

9

10

11

12

13

14

15

16

17

1 Table 7. LR option results. Performance indexes at the Ners, Russan and Remoulins stations.  
 2 The symbols on the right of indexes characterize the gaps compared with the COUPL<sub>MOD</sub>  
 3 option. ↓↓ : Deterioration of more than 50 % ; ↓ : Deterioration between 5 et 50 % ; ↑ :  
 4 Improvement between 5 and 50 % ; ↑↑ : Improvement of more than 50 % ; = : Close values,  
 5 in ± 5 %. Symbol also attributed for RE<sub>Qm</sub>, if the absolute difference is lower in ± 10; and for  
 6 ΔT<sub>Qm</sub>, if the absolute difference is lower in ± 15 minutes.

7

Event	Ners			Russan			Remoulins
	Nash	RE <sub>Qm</sub>	ΔT <sub>Qm</sub>	Nash	RE <sub>Qm</sub>	ΔT <sub>Qm</sub>	ΔT <sub>Qm</sub>
1	0.74 =	-25 =	-50 ↓↓	0.87 =	-7 =	-265 =	45 ↑↑
2	0.62 =	-18 ↓↓	-5 ↑↑	0.61 ↓	-32 ↓↓	-85 ↓↓	-30 =
3	0.93 =	-15 ↓↓	-30 =	0.80 ↓	-36 ↓↓	-70 ↓↓	5 =
4	0.77 =	-13 ↓↓	-10 =	0.73 ↓	-32 ↓↓	-70 ↓↓	-20 =
5	0.78 ↑	-26 =	-45 ↓↓	0.79 ↓	-28 ↓↓	-50 ↓↓	25 =
6	0.62 =	-4 =	15 ↑↑	0.70 =	-18 =	-40 =	5 ↑↑
7	0.77 =	22 ↑	1280 =	0.74 ↓	-4 ↑↑	1245 =	1340 =

8

9

10

11

12

13

14

15

16

17

18

1 Table 8.  $SV_{MOD}$  option results. Performance indexes at the Ners, Russan and Remoulins  
 2 stations. The symbols on the right of indexes characterize the gaps compared with the  
 3  $COUPL_{MOD}$  option.  $\Downarrow\Downarrow$  : Deterioration of more than 50 % ;  $\Downarrow$  : Deterioration between 5 et 50  
 4 % ;  $\Uparrow$  : Improvement between 5 and 50 % ;  $\Uparrow\Uparrow$  : Improvement of more than 50 % ;  $=$  : Close  
 5 values, in  $\pm 5$  %. Symbol also attributed for  $RE_{Qm}$ , if the absolute difference is lower in  $\pm 10$ ;  
 6 and for  $\Delta T_{Qm}$ , if the absolute difference is lower in  $\pm 15$  minutes.

7

Event	Ners			Russan			Remoulins
	Nash	$RE_{Qm}$	$\Delta T_{Qm}$	Nash	$RE_{Qm}$	$\Delta T_{Qm}$	$\Delta T_{Qm}$
1	0.14 $\Downarrow\Downarrow$	-41 $\Downarrow\Downarrow$	140 $\Downarrow\Downarrow$	-0.10 $\Downarrow\Downarrow$	-69 $\Downarrow\Downarrow$	-2510 $\Downarrow\Downarrow$	-2330 $\Downarrow\Downarrow$
2	0.61 $=$	3 $=$	25 $=$	0.72 $=$	-5 $=$	5 $=$	20 $=$
3	0.92 $=$	-5 $=$	25 $=$	0.96 $=$	-11 $=$	-15 $=$	20 $=$
4	0.75 $\Downarrow$	-2 $=$	-15 $=$	0.83 $=$	-14 $=$	-25 $=$	-10 $=$
5	-1.05 $\Downarrow\Downarrow$	-91 $\Downarrow\Downarrow$	255 $\Downarrow\Downarrow$	-0.73 $\Downarrow\Downarrow$	-93 $\Downarrow\Downarrow$	420 $\Downarrow\Downarrow$	-1380 $\Downarrow\Downarrow$
6	0.52 $\Downarrow$	-8 $=$	135 $\Downarrow$	0.51 $\Downarrow$	-25 $\Downarrow\Downarrow$	135 $\Downarrow\Downarrow$	175 $\Downarrow\Downarrow$
7	0.81 $\Uparrow$	27 $\Uparrow$	1315 $=$	0.88 $\Uparrow$	3 $\Uparrow\Uparrow$	1310 $=$	1320 $=$

8

9

10

11

12

1 Table 9. COUPL<sub>MOD</sub> option results. Performance indexes at the Ners, Russan and Remoulins  
2 stations. The symbols on the right of indexes characterize the gaps compared with the  
3 COUPL<sub>MOD</sub> option.  $\downarrow\downarrow$  : Deterioration of more than 50 % ;  $\downarrow$  : Deterioration between 5 et 50  
4 % ;  $\uparrow$  : Improvement between 5 and 50 % ;  $\uparrow\uparrow$  : Improvement of more than 50 % ;  $=$  : Close  
5 values, in  $\pm 5$  %. Symbol also attributed for RE<sub>Qm</sub>, if the absolute difference is lower in  $\pm 10$ ;  
6 and for  $\Delta T_{Qm}$ , if the absolute difference is lower in  $\pm 15$  minutes.

7  
8

Event	Ners			Russan			Remoulins
	Nash	RE <sub>Qm</sub>	$\Delta T_{Qm}$	Nash	RE <sub>Qm</sub>	$\Delta T_{Qm}$	$\Delta T_{Qm}$
1	0.77 =	-25 =	65 $\downarrow\downarrow$	0.89 =	-9 =	-90 =	-195 =
2	0.78 $\uparrow$	5 =	20 =	0.85 $\uparrow$	-6 =	-5 =	15 =
3	0.96 =	9 =	5 =	0.99 =	-2 =	-5 =	0 =
4	0.94 $\uparrow$	5 =	30 =	0.97 $\uparrow$	-8 =	5 $\uparrow\uparrow$	10 =
5	0.63 $\downarrow$	-31 =	-10 =	0.88 =	-14 =	-20 =	-5 =
6	0.95 $\uparrow$	-13 $\downarrow\downarrow$	5 $\uparrow\uparrow$	0.95 $\uparrow$	-12 =	-85 $\downarrow\downarrow$	-70 =
7	0.98 $\uparrow$	12 $\uparrow\uparrow$	15 $\uparrow\uparrow$	0.95 $\uparrow$	3 $\uparrow\uparrow$	5 $\uparrow\uparrow$	-50 $\uparrow\uparrow$

9  
10  
11

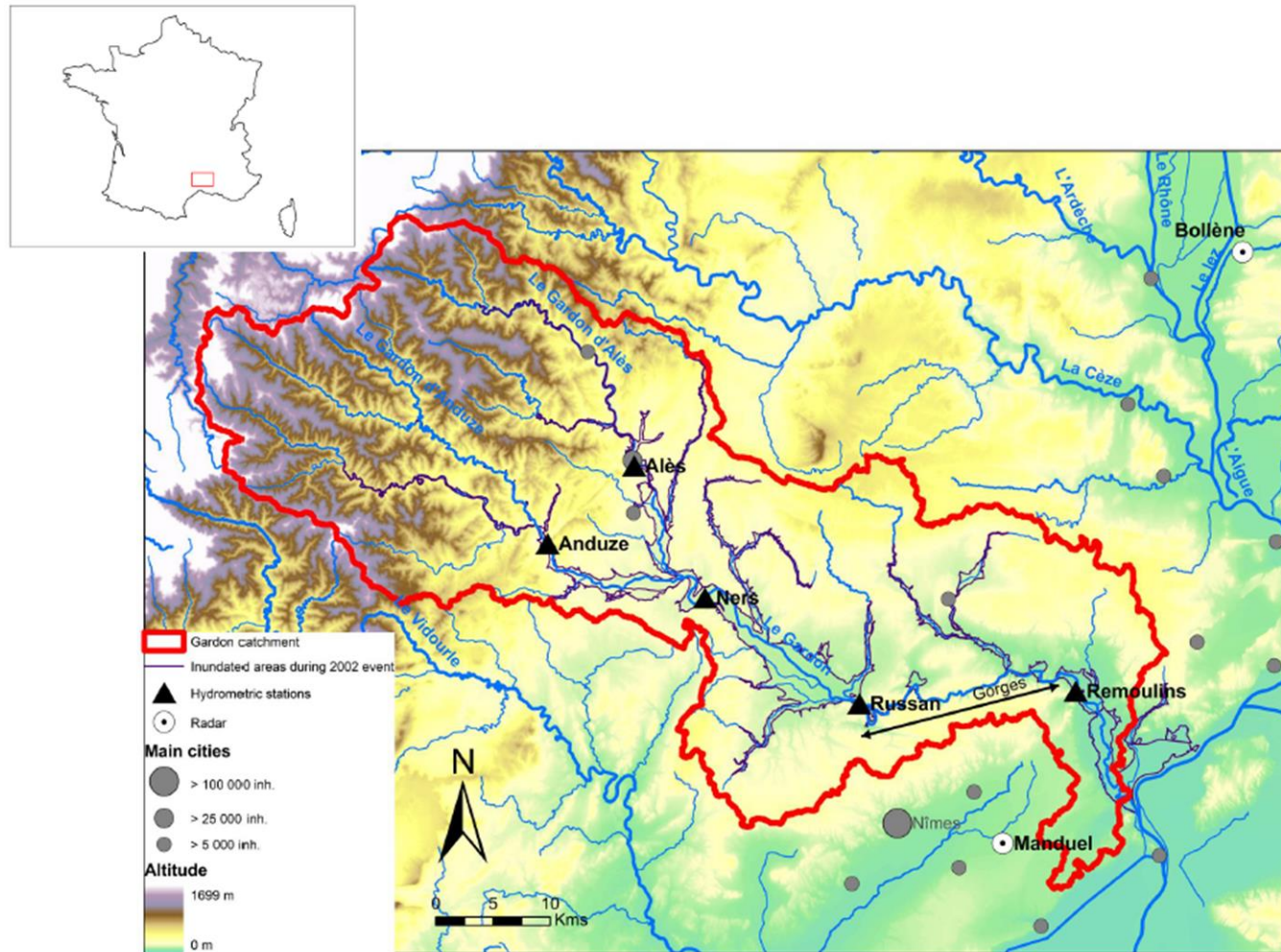
1 Table 10.  $SV_{OBS}$  option results. Performance indexes at the Ners, Russan and Remoulins  
2 stations. The symbols on the right of indexes characterize the gaps compared with the  
3  $COUPL_{MOD}$  option.  $\Downarrow\Downarrow$  : Deterioration of more than 50 % ;  $\Downarrow$  : Deterioration between 5 et 50  
4 % ;  $\Uparrow$  : Improvement between 5 and 50 % ;  $\Uparrow\Uparrow$  : Improvement of more than 50 % ;  $=$  : Close  
5 values, in  $\pm 5$  %. Symbol also attributed for  $RE_{Qm}$ , if the absolute difference is lower in  $\pm 10$ ;  
6 and for  $\Delta T_{Qm}$ , if the absolute difference is lower in  $\pm 15$  minutes.

7

Event	Ners			Russan			Remoulins
	Nash	$RE_{Qm}$	$\Delta T_{Qm}$	Nash	$RE_{Qm}$	$\Delta T_{Qm}$	$\Delta T_{Qm}$
1	0.13 $\Downarrow\Downarrow$	-38 $\Downarrow\Downarrow$	160 $\Downarrow\Downarrow$	-0.10 $\Downarrow\Downarrow$	-67 $\Downarrow\Downarrow$	-2500 $\Downarrow\Downarrow$	-2315 $\Downarrow\Downarrow$
2	0.78 $\Uparrow$	3 =	20 =	0.85 $\Uparrow$	-7 =	-10 =	15 =
3	0.96 =	0 =	15 =	0.97 =	-10 =	-15 =	10 =
4	0.89 $\Uparrow$	3 =	35 =	0.94 $\Uparrow$	-10 =	5 $\Uparrow\Uparrow$	15 =
5	-1.14 $\Downarrow\Downarrow$	-94 $\Downarrow\Downarrow$	220 $\Downarrow\Downarrow$	-0.75 $\Downarrow\Downarrow$	-96 $\Downarrow\Downarrow$	480 $\Downarrow\Downarrow$	430 $\Downarrow\Downarrow$
6	0.86 $\Uparrow$	-26 $\Downarrow\Downarrow$	-590 $\Downarrow\Downarrow$	0.77 $\Uparrow$	-39 $\Downarrow\Downarrow$	-590 $\Downarrow\Downarrow$	-530 $\Downarrow\Downarrow$
7	0.91 $\Uparrow$	8 $\Uparrow\Uparrow$	-5 $\Uparrow\Uparrow$	0.87 $\Uparrow$	-9 =	-45 $\Uparrow\Uparrow$	-55 $\Uparrow\Uparrow$

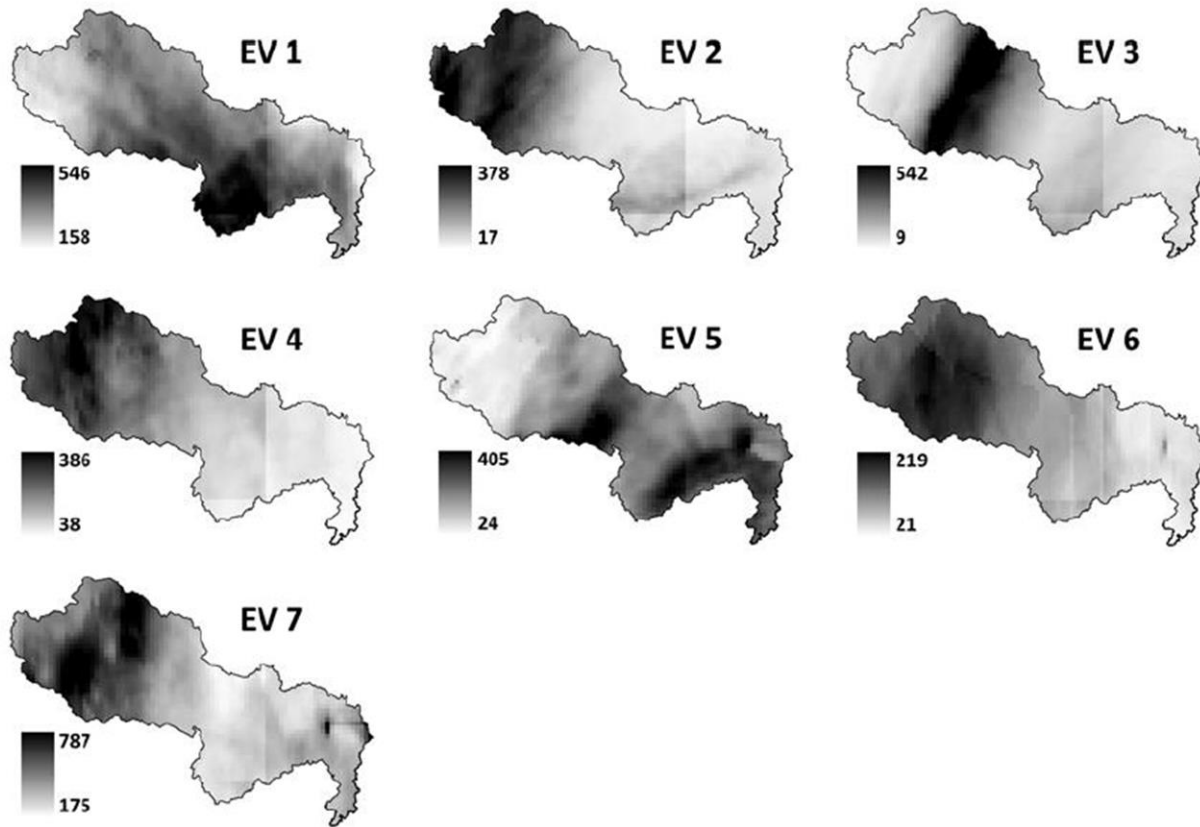
8

1 Figure 1. The Gardon catchment.



2

1 Figure 2. Cumulated rainfall (mm) for each event.

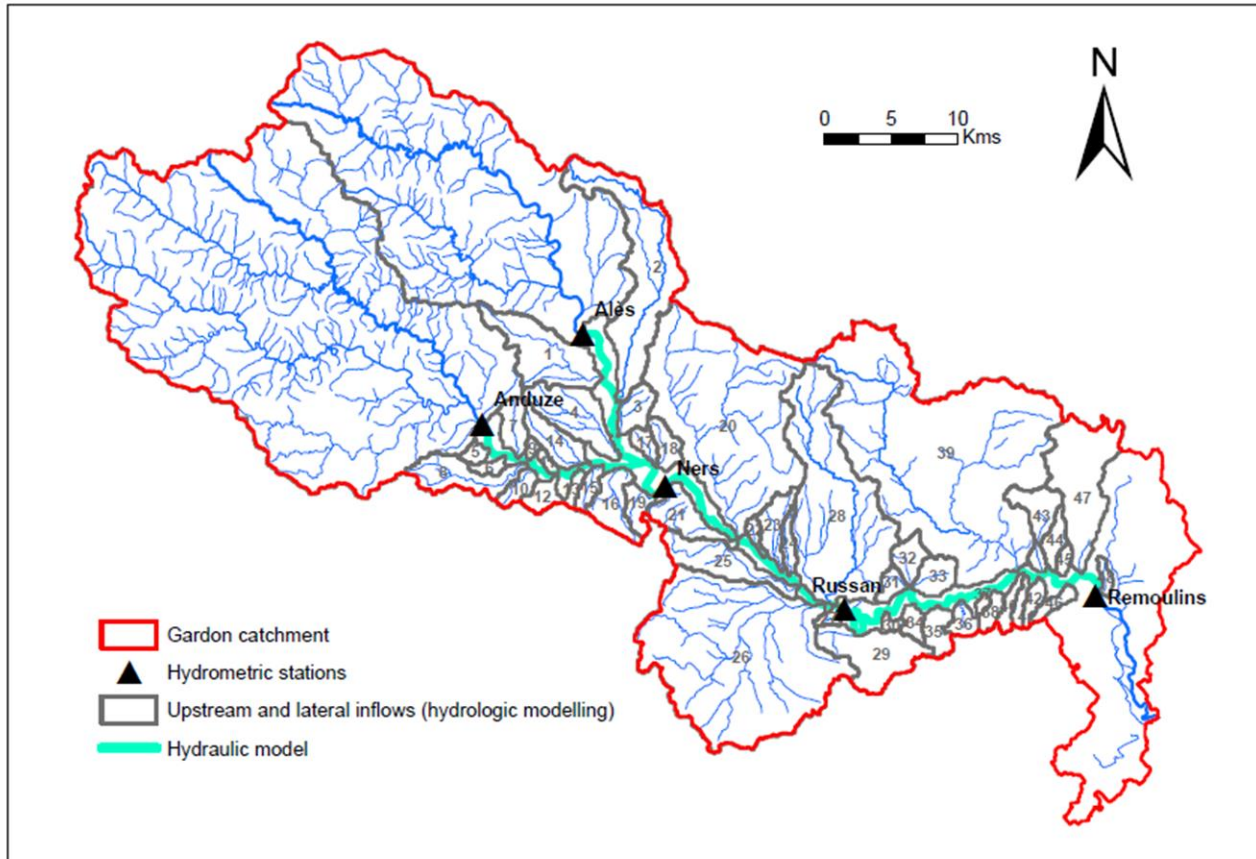


2

3

1 Figure 3. Coupling of models applied to the Gardon river basin.

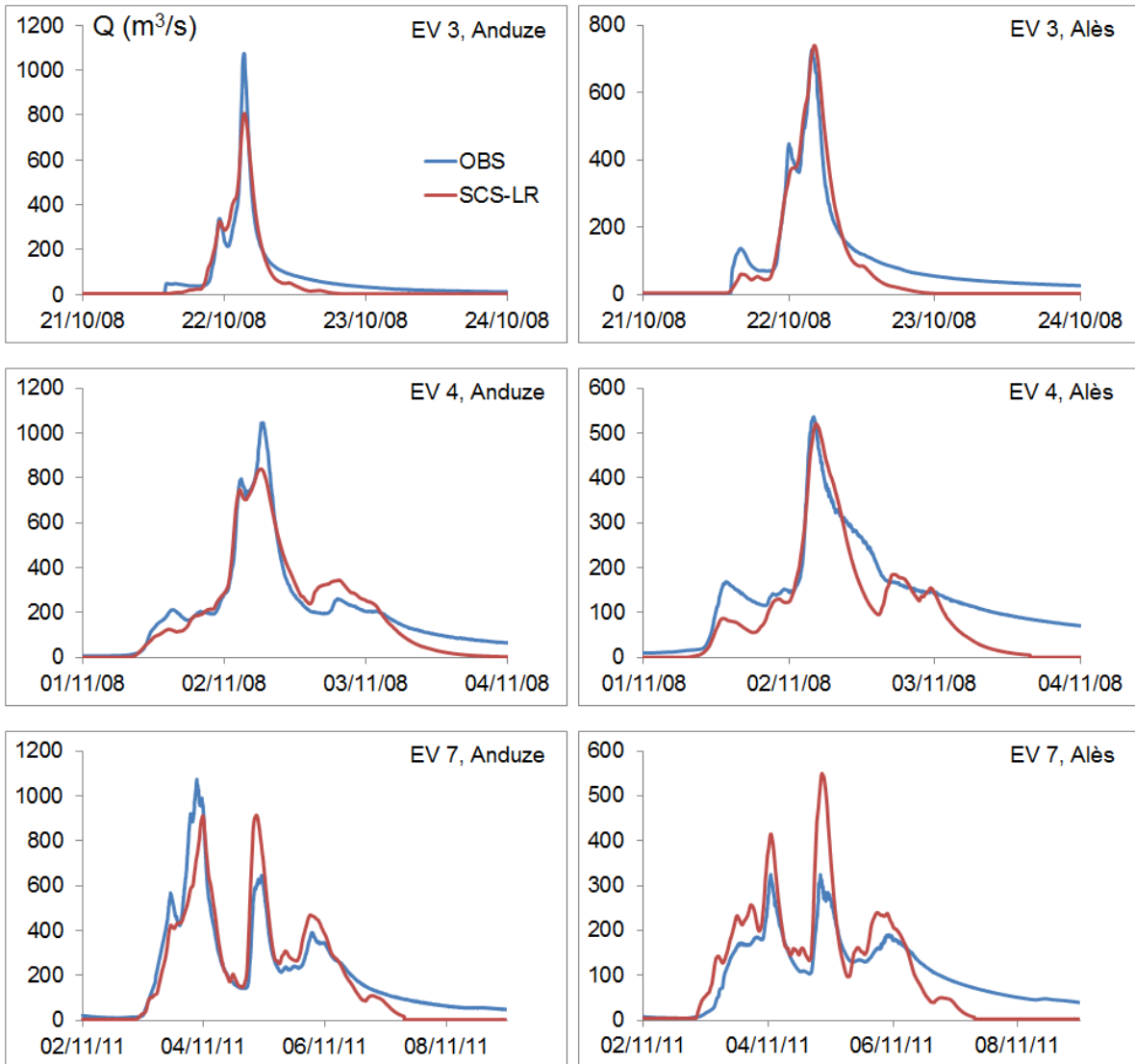
2



3

1 Figure 4. Hydrographs modelled (with SCS-LR) for events n°3, 4, and 7 at the Anduze and  
2 Alès stations.

3



4

5

6

7

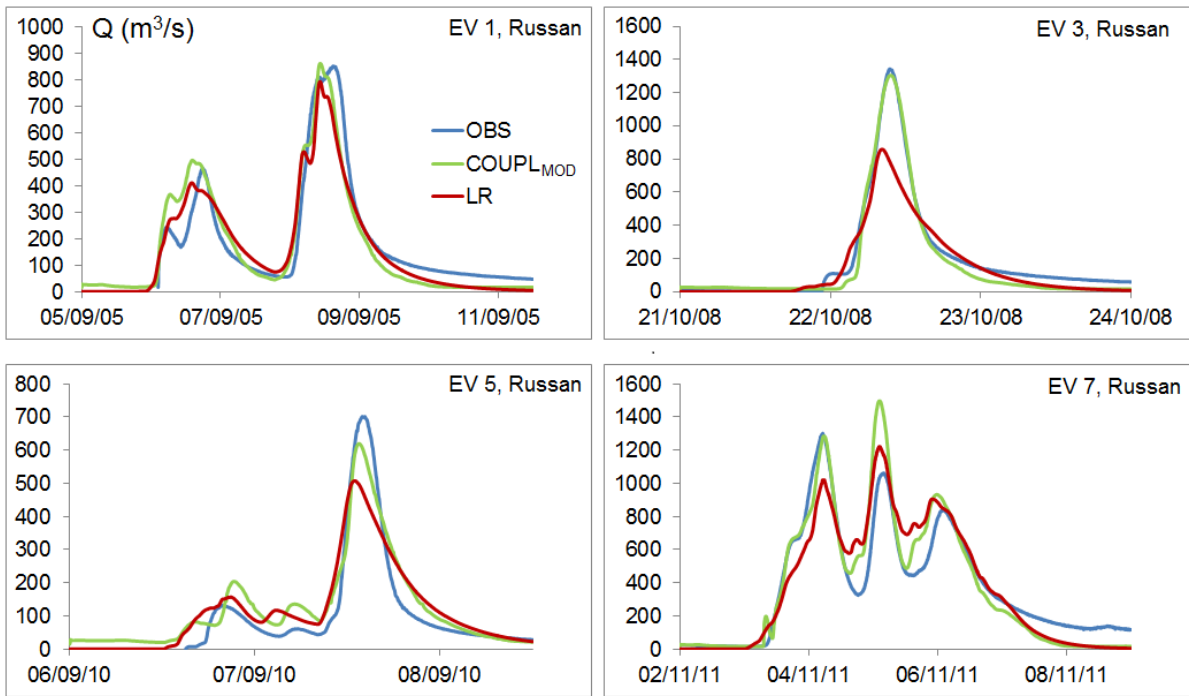
8

9

10

1 Figure 5. Hydrographs modelled for events n°1, 3, 5 and 7 according to COUPL<sub>MOD</sub> and LR  
2 modelling options, at the Russian station.

3



4

5

6

7

8

9

10

11

12

13

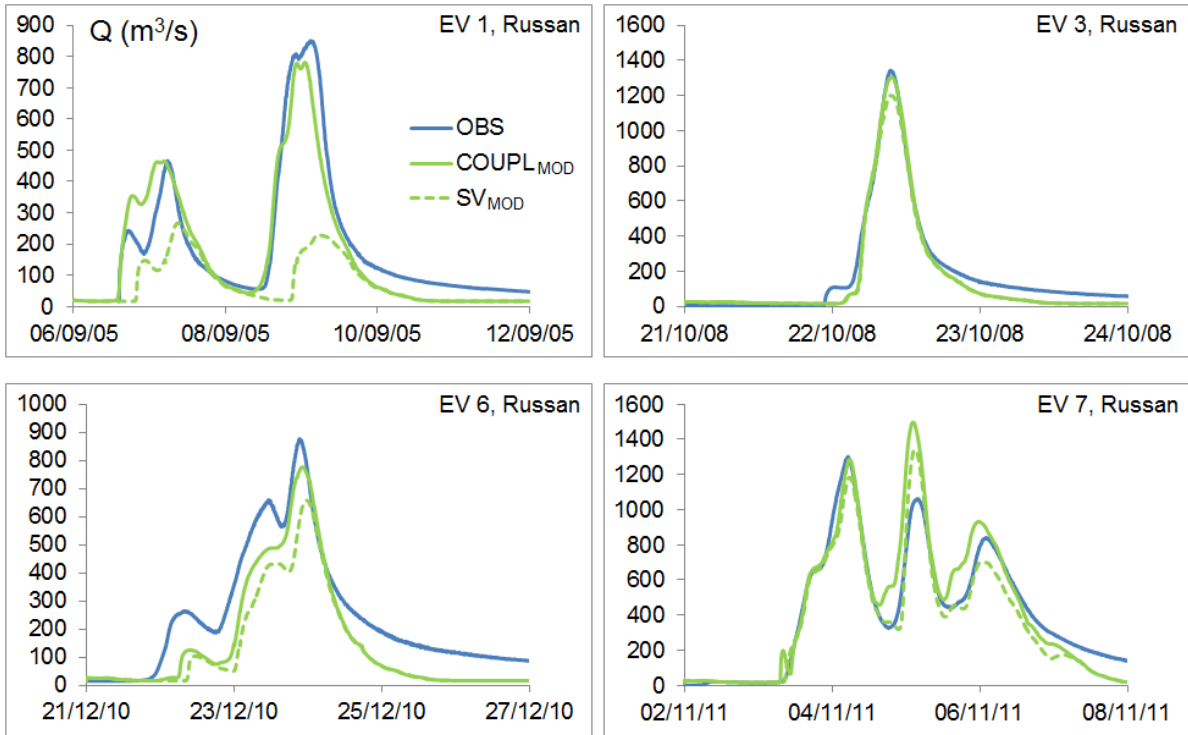
14

15

16

1 Figure 6. Hydrographs modelled for events n°1, 3, 6 and 7 according to COUPL<sub>MOD</sub> and  
2 SV<sub>MOD</sub> modelling options, at the Russan station.

3



4

5

6

7

8

9

10

11

12

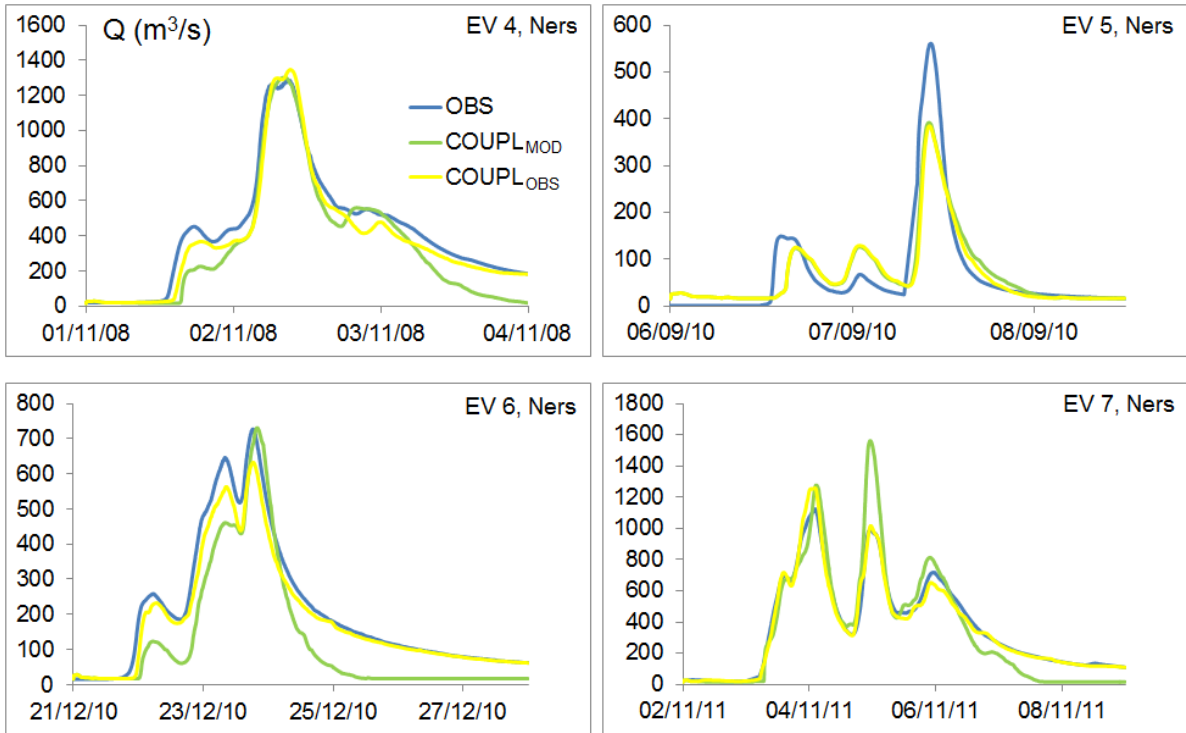
13

14

15

1 Figure 7. Hydrographs modelled for events n°4, 5, 6 and 7 according to COUPL<sub>MOD</sub> and  
2 COUPL<sub>OBS</sub> modelling options, at the Ners station.

3



4

5

6

7

8

9

10

11

12

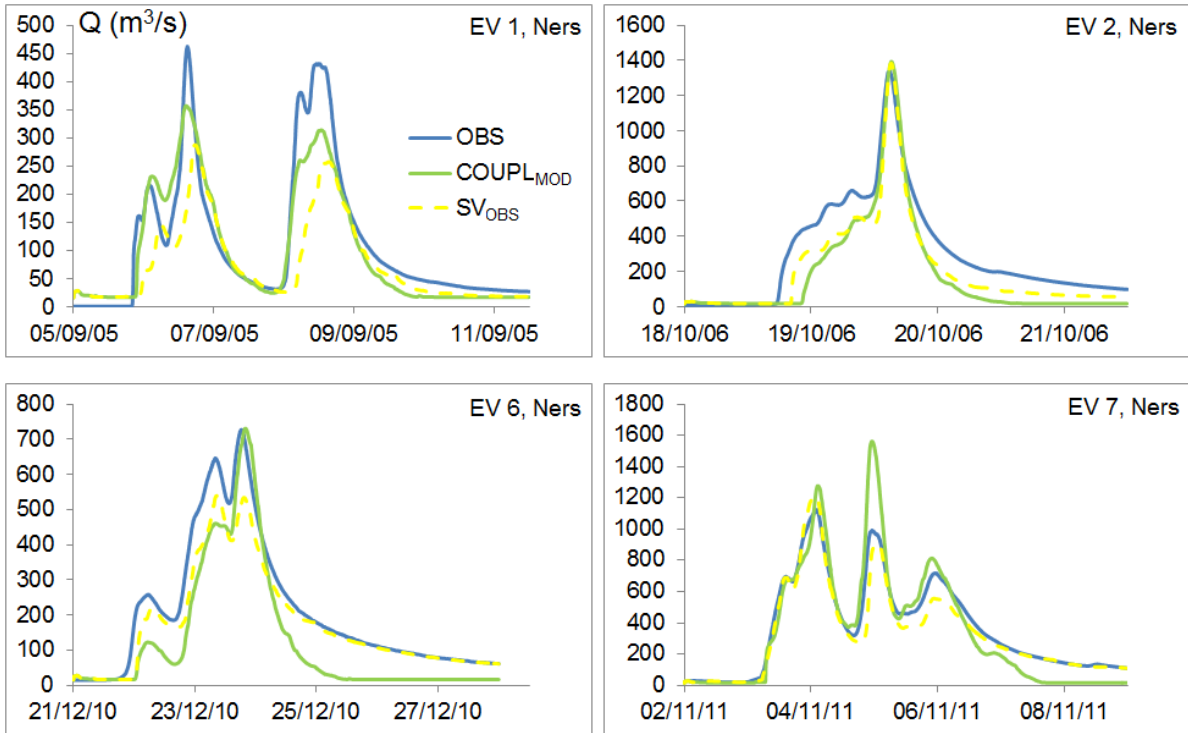
13

14

15

1 Figure 8. Hydrographs modelled for events n°1, 2, 6 and 7 according to COUPL<sub>MOD</sub> and  
2 SV<sub>OBS</sub> modelling options, at the Ners station.

3



4

5